

# Inertia-Free Spacecraft Attitude Control Using Reaction Wheels

Avishai Weiss,\* Ilya Kolmanovsky,† and Dennis S. Bernstein‡  
 University of Michigan, Ann Arbor, Michigan 48109-2140

and

Amit Sanyal‡

New Mexico State University, Las Cruces, New Mexico 88003-8001

DOI: 10.2514/1.58363

**This paper extends the continuous inertia-free control law for spacecraft attitude tracking derived in prior work to the case of three axisymmetric reaction wheels. The wheels are assumed to be mounted in a known and linearly independent, but not necessarily orthogonal, configuration with an arbitrary and unknown orientation relative to the unknown spacecraft principal axes. Simulation results for slew and spin maneuvers are presented with torque and momentum saturation.**

## I. Introduction

**I**N SPACECRAFT applications, it is often expensive to determine the mass properties with a high degree of accuracy. To alleviate this requirement, the control algorithms given in [1–3] are inertia free in the sense that they require no prior modeling of the mass distribution. The control algorithms in [2,3] incorporate internal states that can be viewed as estimates of the moments and products of inertia; however, these estimates need not converge to the true values and in fact do not converge to the true values except under sufficiently persistent motion.

The results of [3] are based on rotation matrices [4] as an alternative to the quaternions as used in [2,5,6]. Quaternions provide a double cover of the rotation group  $SO(3)$  and, thus, when used as the basis of a continuous control algorithm, cause unwinding that is unnecessary rotation away from and then back to the desired physical attitude [7]. To avoid unwinding while using quaternions, it is thus necessary to resort to discontinuous control algorithms, which introduce the possibility of chatter due to noise as well as mathematical complications [8–10]. On the other hand, rotation matrices allow for continuous control laws but introduce multiple equilibria. Because the spurious equilibria of the closed-loop system are saddle points, the attitude of the spacecraft converges almost globally (but not globally) to the desired equilibrium. Although the derivation of the inertia-free controller in [3] and the present paper is based on rotation matrices, the relevant attitude error given by the  $S$  parameter [see Eq. (42)] can be computed from any attitude parameterization, such as quaternions or modified Rodrigues parameters, and thus, the continuous inertia-free controllers presented in [3] are not confined to rotation matrices.

The inertia-free control laws in [1–3] assume that three-axis input torques can be specified without onboard momentum storage, which implies implementation in terms of thrusters. However, attitude control laws are typically implemented with wheels, and thus, the onboard stored momentum varies with time. To account for this effect, the contribution of this paper is the derivation of an inertia-free control law based on reaction-wheel actuation. Like the inertia-free control laws in [1–3], the tuning of this control law requires no

knowledge of the mass properties of the spacecraft, and this paper specifies the assumptions and modeling information concerning the reaction wheels and their placement relative to the bus.

The paper is organized as follows. In Sec. II, coordinate-free equations of motion for the spacecraft are derived, in which, unlike [11], the present paper does not assume that the wheels are aligned with the principal axes of the spacecraft bus nor does it assume that the wheels are balanced with respect to the bus in order to preserve the location of its center of mass; in fact, the reaction wheels may be mounted at any location and in any linearly independent configuration. In Sec. III, the control objectives are formulated, and in Sec. IV, the controller is developed. Simulation results are reported in Sec. V, in which the robustness to variations in the spacecraft inertia is demonstrated and controller performance is examined under both torque and momentum saturation. Finally, concluding remarks are made in Sec. VI.

## II. Spacecraft Model with Reaction Wheels

This section derives the equations of motion for a spacecraft with reaction wheels, while highlighting the underlying assumptions on wheel geometry, inertia, and attachment to the bus. Throughout the paper, the vector  $\mathbf{r}_{q/p}$  denotes the position of point  $q$  relative to point  $p$ , the vector  $\mathbf{v}_{q/p/X} = \dot{\mathbf{r}}_{q/p}$  denotes the velocity of point  $q$  relative to point  $p$  with respect to frame  $F_X$ , and the vector  $\boldsymbol{\omega}_{Y/X}$  denotes the angular velocity of frame  $F_Y$  relative to frame  $F_X$ . Note that  $(\cdot)$  denotes a coordinate-free (unresolved) vector. All frames are orthogonal and right handed.

*Definition 1:* Let  $F_X$  be a frame, let  $\mathcal{B}$  be a collection of rigid bodies  $\mathcal{B}_1, \dots, \mathcal{B}_l$ , and let  $p$  be a point. Then, the angular momentum of  $\mathcal{B}$  relative to  $p$  with respect to  $F_X$  is defined by

$$\mathbf{H}_{\mathcal{B}/p/X} \triangleq \sum_{i=1}^l \mathbf{H}_{\mathcal{B}_i/p/X} \quad (1)$$

where, for  $i = 1, \dots, l$ , the angular momentum  $\mathbf{H}_{\mathcal{B}_i/p/X}$  of  $\mathcal{B}_i$  relative to  $p$  with respect to  $F_X$  is defined by

$$\mathbf{H}_{\mathcal{B}_i/p/X} \triangleq \int_{\mathcal{B}_i} \mathbf{r}_{dm/p} \times \mathbf{v}_{dm/p/X} dm \quad (2)$$

The following properties of angular momentum are standard [12].

*Lemma 1:* Let  $\mathcal{B}$  be a rigid body, let  $F_X$  and  $F_Y$  be frames, and let  $p$  be a point. Then,

$$\mathbf{H}_{\mathcal{B}/p/X} = \mathbf{I}_{\mathcal{B}/p} \boldsymbol{\omega}_{Y/X} + \mathbf{H}_{\mathcal{B}/p/Y} \quad (3)$$

where the positive-definite coordinate-free inertia tensor  $\mathbf{I}_{\mathcal{B}/p}$  is defined by

Presented as Paper 2010-8297 at the AIAA Guidance Navigation and Control Conference, Toronto, 2–5 August 2010; received 20 March 2012; revision received 12 January 2013; accepted for publication 8 February 2013; published online 19 July 2013. Copyright © 2013 by Avishai Weiss. Published by the American Institute of Aeronautics and Astronautics, Inc., with permission. Copies of this paper may be made for personal or internal use, on condition that the copier pay the \$10.00 per-copy fee to the Copyright Clearance Center, Inc., 222 Rosewood Drive, Danvers, MA 01923; include the code 1533-3884/13 and \$10.00 in correspondence with the CCC.

\*Graduate Student, Department of Aerospace Engineering.

†Professor, Department of Aerospace Engineering. Member AIAA.

‡Assistant Professor, Department of Mechanical and Aerospace Engineering. Member AIAA.

$$\mathbf{I}_{B/p} \triangleq \int_B |\mathbf{r}_{dm/p}|^2 \mathbf{U} - \mathbf{r}_{dm/p} \mathbf{r}'_{dm/p} \, dm \quad (4)$$

and where  $\mathbf{U}$  denotes the second-order identity tensor.

*Lemma 2:* Let  $\mathcal{B}$  be a rigid body, let  $F_X$  and  $F_Y$  be frames, let  $F_Y$  be a body-fixed frame, and let  $p$  be a point that is fixed in  $\mathcal{B}$ . Then,

$$\mathbf{H}_{B/p/Y} = 0 \quad (5)$$

and

$$\mathbf{H}_{B/p/X} = \mathbf{I}_{B/p} \boldsymbol{\omega}_{Y/X} \quad (6)$$

*Lemma 3:* Let  $F_X$  be a frame, let  $p$  be a point, let  $\mathcal{B}$  be a rigid body with mass  $m_B$ , and let  $c$  be the center of mass of  $\mathcal{B}$ . Then,

$$\mathbf{H}_{B/p/X} = \mathbf{H}_{B/c/X} + \mathbf{r}_{c/p} \times m_B \mathbf{v}_{c/p/X} \quad (7)$$

Consider a spacecraft  $sc$  actuated by three axisymmetric wheels  $w_1, w_2, w_3$  attached to a rigid bus  $b$  in a known and linearly independent, but not necessarily orthogonal, configuration. Although the spacecraft is not a rigid body, the axial symmetry of the wheels implies that the center of mass  $c$  of the spacecraft is fixed in both the bus and the spacecraft. Because the inertia properties of the bus are assumed to be unknown, the principal axes of the bus are unknown, and thus, the wheel configuration has an arbitrary and unknown orientation relative to the principal axes of the bus. Each wheel is mounted so that it rotates about one of its own principal axes passing through its own center of mass. It is not assumed that the axis of rotation of each wheel passes through the center of mass of the bus, nor is it assumed that the wheels are balanced with respect to the bus in order to preserve the location of its center of mass. Thus, the center of mass of the spacecraft and the center of mass of the bus may be distinct points, both of which are unknown.

Assume a bus-fixed frame  $F_B$ ; three wheel-fixed frames  $F_{w_1}, F_{w_2}, F_{w_3}$ , for which the  $x$  axes are aligned with the rotation axes of  $w_1, w_2, w_3$ , respectively; and an Earth-centered inertial frame  $F_E$ . The angular momentum of the spacecraft relative to its center of mass with respect to the inertial frame is given by

Definition 1:

$$\mathbf{H}_{sc/c/E} = \mathbf{H}_{b/c/E} + \sum_{i=1}^3 \mathbf{H}_{w_i/c/E} \quad (8)$$

where the angular momentum  $\mathbf{H}_{b/c/E}$  of the bus relative to  $c$  with respect to  $F_E$  is given by

Lemma 2:

$$\mathbf{H}_{b/c/E} = \mathbf{I}_{b/c} \boldsymbol{\omega}_{B/E} \quad (9)$$

where  $\mathbf{I}_{b/c}$  is the positive-definite inertia tensor of the bus relative to the center of mass of the spacecraft, and  $\boldsymbol{\omega}_{B/E}$  is the angular velocity of  $F_B$  with respect to  $F_E$ . The angular momentum  $\mathbf{H}_{w_i/c/E}$  of wheel  $i$  relative to the center of mass of the spacecraft with respect to the inertial frame is given by

Lemma 1:

$$\mathbf{H}_{w_i/c/E} = \mathbf{I}_{w_i/c} \boldsymbol{\omega}_{B/E} + \mathbf{H}_{w_i/c/B}$$

Lemma 3:

$$= \mathbf{I}_{w_i/c} \boldsymbol{\omega}_{B/E} + \mathbf{H}_{w_i/c_i/B} + \mathbf{r}_{c_i/c} \times m_{w_i} \mathbf{v}_{c_i/c/B}$$

Lemma 2:

$$= \mathbf{I}_{w_i/c} \boldsymbol{\omega}_{B/E} + \mathbf{I}_{w_i/c_i} \boldsymbol{\omega}_{w_i/B} \quad (10)$$

where  $\mathbf{I}_{w_i/c}$  is the inertia tensor of wheel  $i$  relative to the center of mass of the spacecraft,  $\mathbf{I}_{w_i/c_i}$  is the inertia tensor of wheel  $i$  relative to the center of mass  $c_i$  of the  $i$ th wheel, and  $\boldsymbol{\omega}_{w_i/B}$  is the angular velocity of wheel  $i$  relative to the bus. Thus, Eq. (8) is given by

$$\mathbf{H}_{sc/c/E} = \left( \mathbf{I}_{b/c} + \sum_{i=1}^3 \mathbf{I}_{w_i/c} \right) \boldsymbol{\omega}_{B/E} + \sum_{i=1}^3 \mathbf{I}_{w_i/c_i} \boldsymbol{\omega}_{w_i/B} \quad (11)$$

Resolving  $\boldsymbol{\omega}_{w_i/B}$  in  $F_{w_i}$  yields

$$\boldsymbol{\omega}_{w_i/B}|_{w_i} = \psi_i e_1 \quad (12)$$

where  $e_1 = [1 \ 0 \ 0]^T$  and  $\psi_i$  is the angular rate relative to  $F_B$  of the  $i$ th wheel about the  $x$  axis of  $F_{w_i}$ . Because  $F_{w_i}$  is aligned with the principal axes of wheel  $i$ , it follows that

$$\mathbf{I}_{w_i/c_i}|_{w_i} = \text{diag}(\alpha_i, \beta_i, \beta_i) \quad (13)$$

Note that  $\boldsymbol{\omega}_{w_i/B}$  is an eigenvector of  $\mathbf{I}_{w_i/c_i}$  with eigenvalue  $\alpha_i$ ; that is,  $\mathbf{I}_{w_i/c_i} \boldsymbol{\omega}_{w_i/B} = \alpha_i \boldsymbol{\omega}_{w_i/B}$ .

### A. Spacecraft Equations of Motion

The equations of motion for a spacecraft with reaction wheels as described before are now derived. It follows from Newton's second law for rotation that

$$\begin{aligned} \mathbf{M}_{sc/c} &= \overset{E\bullet}{\mathbf{H}}_{sc/c/E} = \left( \mathbf{I}_{b/c} + \sum_{i=1}^3 \mathbf{I}_{w_i/c} \right) \boldsymbol{\omega}_{B/E} + \sum_{i=1}^3 \mathbf{I}_{w_i/c_i} \boldsymbol{\omega}_{w_i/B} \\ &= \left( \mathbf{I}_{b/c} + \sum_{i=1}^3 \mathbf{I}_{w_i/c} \right) \boldsymbol{\omega}_{B/E} + \boldsymbol{\omega}_{B/E} \times \left( \mathbf{I}_{b/c} + \sum_{i=1}^3 \mathbf{I}_{w_i/c} \right) \boldsymbol{\omega}_{B/E} \\ &\quad + \sum_{i=1}^3 \mathbf{I}_{w_i/c_i} \boldsymbol{\omega}_{w_i/B} + \boldsymbol{\omega}_{B/E} \times \sum_{i=1}^3 \mathbf{I}_{w_i/c_i} \boldsymbol{\omega}_{w_i/B} \\ &= \left( \mathbf{I}_{b/c} + \sum_{i=1}^3 \mathbf{I}_{w_i/c} \right) \overset{B\bullet}{\boldsymbol{\omega}}_{B/E} + \sum_{i=1}^3 \alpha_i \overset{B\bullet}{\boldsymbol{\omega}}_{w_i/B} \\ &\quad + \boldsymbol{\omega}_{B/E} \times \left( \left( \mathbf{I}_{b/c} + \sum_{i=1}^3 \mathbf{I}_{w_i/c} \right) \boldsymbol{\omega}_{B/E} + \sum_{i=1}^3 \alpha_i \boldsymbol{\omega}_{w_i/B} \right) \end{aligned} \quad (14)$$

To resolve Eq. (14) in  $F_B$ , the following notation is used:

$$\begin{aligned} J_b &\triangleq \mathbf{I}_{b/c}|_B, & J_{w_i} &\triangleq \mathbf{I}_{w_i/c}|_B, & J_w &\triangleq \sum_{i=1}^3 \mathbf{I}_{w_i/c}|_B, \\ J_{sc} &\triangleq J_b + J_w, & \boldsymbol{\omega} &\triangleq \boldsymbol{\omega}_{B/E}|_B, & \dot{\boldsymbol{\omega}} &\triangleq \overset{B\bullet}{\boldsymbol{\omega}}_{B/E}|_B, & \nu_i &\triangleq \boldsymbol{\omega}_{w_i/B}|_B, \\ & & \dot{\nu}_i &\triangleq \overset{B\bullet}{\boldsymbol{\omega}}_{w_i/B}|_B, & \tau_{\text{dist}} &\triangleq \mathbf{M}_{sc/c}|_B \end{aligned}$$

The vector  $\tau_{\text{dist}}$  represents the disturbance torques, that is, all external torques applied to the spacecraft aside from control torques. Disturbance torques may be due to gravity gradients, solar pressure, atmospheric drag, or the ambient magnetic field.

As in Eq. (12), the angular acceleration  $\dot{\nu}_i$  of each wheel has one degree of freedom. In  $F_{w_i}$ ,

$$\overset{B\bullet}{\boldsymbol{\omega}}_{w_i/B}|_{w_i} = \overset{w_i\bullet}{\boldsymbol{\omega}}_{w_i/B}|_{w_i} = \dot{\psi}_i e_1 \quad (15)$$

Thus,

$$\dot{\nu}_i = \overset{B\bullet}{\boldsymbol{\omega}}_{w_i/B}|_B = \mathcal{O}_{B/w_i} \overset{B\bullet}{\boldsymbol{\omega}}_{w_i/B}|_{w_i} = \mathcal{O}_{B/w_i} \dot{\psi}_i e_1 \quad (16)$$

where the proper orthogonal matrix  $\mathcal{O}_{B/W_i} \in \mathbb{R}^{3 \times 3}$  is the orientation matrix that transforms components of a vector resolved in  $F_{W_i}$  into the components of the same vector resolved in  $F_B$ .

With the preceding notation, resolving Eq. (14) in  $F_B$  yields

$$\begin{aligned} \tau_{\text{dist}} &= (J_b + J_w)\dot{\omega} + \sum_{i=1}^3 \alpha_i \dot{\nu}_i + \omega \times \left( (J_b + J_w)\omega + \sum_{i=1}^3 \alpha_i \nu_i \right) \\ &= J_{\text{sc}}\dot{\omega} + \sum_{i=1}^3 \alpha_i \mathcal{O}_{B/W_i} \dot{\psi}_i e_1 + \omega \times \left( J_{\text{sc}}\omega + \sum_{i=1}^3 \alpha_i \mathcal{O}_{B/W_i} \psi_i e_1 \right) \\ &= J_{\text{sc}}\dot{\omega} + J_\alpha \dot{\nu} + \omega \times (J_{\text{sc}}\omega + J_\alpha \nu) \end{aligned} \quad (17)$$

where

$$J_\alpha \triangleq [\alpha_1 \mathcal{O}_{B/W_1} e_1 \quad \alpha_2 \mathcal{O}_{B/W_2} e_1 \quad \alpha_3 \mathcal{O}_{B/W_3} e_1] \quad (18)$$

$\nu \triangleq [\nu_1 \quad \nu_2 \quad \nu_3]^T$ , and  $\dot{\nu} \triangleq [\dot{\nu}_1 \quad \dot{\nu}_2 \quad \dot{\nu}_3]^T$ . Rearranging Eq. (17) and choosing the control input  $u$  to be  $\dot{\nu}$  yields the equations of motion for a spacecraft with reaction wheels, which have the form

$$J_{\text{sc}}\dot{\omega} = (J_{\text{sc}}\omega + J_\alpha \nu) \times \omega - J_\alpha u + \tau_{\text{dist}} \quad (19)$$

$$\dot{\nu} = u \quad (20)$$

In practice, a servo loop is closed around each reaction wheel in order to produce the desired wheel angular accelerations given in Eq. (20).

Instead of commanding wheel angular accelerations by implementing servo loops, motor torque commands can be used. To determine the relationship between the desired angular acceleration and the required motor torque, the dynamic equations for each wheel must be derived. It follows that

$$\begin{aligned} M_{W_i/c_i} &= \overset{E \bullet}{\mathbf{H}}_{W_i/c_i/E} \\ &= \overbrace{\mathbf{I}_{W_i/c_i} \omega_{W_i/E}}^E \\ &= \mathbf{I}_{W_i/c_i} \overset{W \bullet}{\omega}_{W_i/E} + \omega_{W_i/E} \times \mathbf{I}_{W_i/c_i} \omega_{W_i/E} \\ &= \mathbf{I}_{W_i/c_i} (\overset{B \bullet}{\omega}_{B/E} + \overset{B \bullet}{\omega}_{W_i/B} - \omega_{W_i/B} \times \omega_{B/E}) \\ &\quad + (\omega_{B/E} + \omega_{W_i/B}) \times \mathbf{I}_{W_i/c_i} (\omega_{B/E} + \omega_{W_i/B}) \end{aligned} \quad (21)$$

Resolving Eq. (21) in  $F_B$  and projecting it along each motor axis yields

$$\tau_{\text{motor},i} = e_i^T [J_{W_i/c_i} (\dot{\omega} + \dot{\nu}_i - \nu_i \times \omega) + (\omega + \nu_i) \times J_{W_i/c_i} (\omega + \nu_i)] \quad (22)$$

where  $J_{W_i/c_i} \triangleq \mathbf{I}_{W_i/c_i}|_B$ . Although Eq. (22) can be used for torque control, the measurements of  $\omega$ ,  $\dot{\omega}$ ,  $\nu_i$ , and  $\dot{\nu}_i$  needed to implement it demonstrate why reaction wheels are typically angular-acceleration commanded and feedback controlled rather than torque commanded.

### B. Specialization: Principal-Axis Alignment

As in [11], the equations of motion (19) and (20) are now specialized by assuming that the principal axes of the bus are aligned with the rotational axes of the wheels; that the wheels are mass balanced relative to the center of mass of the bus so that the center of mass of the spacecraft coincides with the center of mass of the bus; and, finally, that the moments of inertia  $\beta_1, \beta_2, \beta_3$  of the wheels are lumped into the bus inertia  $J_b = \text{diag}(J_{b_1}, J_{b_2}, J_{b_3})$ , where  $J_{b_1} \triangleq J_b + \beta_2 + \beta_3$ ,  $J_{b_2} \triangleq J_b + \beta_1 + \beta_3$  and  $J_{b_3} \triangleq J_b + \beta_1 + \beta_2$ . In this configuration,

$$\mathcal{O}_{B/W_1} e_1 = \begin{bmatrix} 1 \\ 0 \\ 0 \end{bmatrix}, \quad \mathcal{O}_{B/W_2} e_1 = \begin{bmatrix} 0 \\ 1 \\ 0 \end{bmatrix}, \quad \mathcal{O}_{B/W_3} e_1 = \begin{bmatrix} 0 \\ 0 \\ 1 \end{bmatrix} \quad (23)$$

Therefore,  $J_\alpha = J_w = \text{diag}(\alpha_1, \alpha_2, \alpha_3)$ . Rewriting the equations of motion (19) and (20) as

$$J_b \dot{\omega} = ((J_b + J_\alpha)\omega + J_\alpha \nu) \times \omega + u + \tau_{\text{dist}} \quad (24)$$

$$-u = J_\alpha (\dot{\omega} + \dot{\nu}) \quad (25)$$

and simplifying yields

$$\begin{aligned} J_{b_1} \dot{\omega}_1 &= (J_{b_2} - J_{b_3})\omega_2\omega_3 + \alpha_2\omega_3(\omega_2 + \nu_2) \\ &\quad - \alpha_3\omega_2(\omega_3 + \nu_3) + u_1 + \tau_{\text{dist}_1} \end{aligned} \quad (26)$$

$$\begin{aligned} J_{b_2} \dot{\omega}_2 &= (J_{b_3} - J_{b_1})\omega_3\omega_1 + \alpha_3\omega_1(\omega_3 + \nu_3) \\ &\quad - \alpha_1\omega_3(\omega_1 + \nu_1) + u_2 + \tau_{\text{dist}_2} \end{aligned} \quad (27)$$

$$\begin{aligned} J_{b_3} \dot{\omega}_3 &= (J_{b_1} - J_{b_2})\omega_1\omega_2 + \alpha_1\omega_2(\omega_1 + \nu_1) \\ &\quad - \alpha_2\omega_1(\omega_2 + \nu_2) + u_3 + \tau_{\text{dist}_3} \end{aligned} \quad (28)$$

$$-u_1 = \alpha_1 (\dot{\omega}_1 + \dot{\nu}_1) \quad (29)$$

$$-u_2 = \alpha_2 (\dot{\omega}_2 + \dot{\nu}_2) \quad (30)$$

$$-u_3 = \alpha_3 (\dot{\omega}_3 + \dot{\nu}_3) \quad (31)$$

which are Eqs. (7.59) and (7.60) of [11].

### III. Spacecraft Model, Assumptions, and Control Objectives

For the control laws (44) and (53) given next, the assumptions presented in Sec. II.B are not invoked. The kinematics of the spacecraft are given by Poisson's equation

$$\dot{R} = R\omega^\times \quad (32)$$

which complements Eqs. (19) and (20). In Eq. (32),  $\omega^\times$  denotes the skew-symmetric matrix of  $\omega$ , and  $R \triangleq \mathcal{O}_{E/B} \in \mathbb{R}^{3 \times 3}$ . Both rate (inertial) and attitude (noninertial) measurements are assumed to be available.

Compared to the case of thrusters treated in [3], reaction-wheel actuation complicates the dynamic equations due to the term  $J_\alpha \nu$  in Eq. (19), as well as the integrators (20) augmented to the system. The kinematic relation (32) remains unchanged. The torque inputs applied to each reaction wheel are constrained by current limitations on the electric motors and amplifiers as well as angular-velocity constraints on the wheels. These constraints are addressed indirectly in Sec. V.

The objective of the attitude control problem is to determine control inputs such that the spacecraft attitude given by  $R$  follows a commanded attitude trajectory given by a possibly time-varying  $C^1$  rotation matrix  $R_d(t)$ . For  $t \geq 0$ ,  $R_d(t)$  is given by

$$\dot{R}_d(t) = R_d(t)\omega_d(t)^\times \quad (33)$$

$$R_d(0) = R_{d0} \quad (34)$$

where  $\omega_d$  is the desired, possibly time-varying angular velocity. The error between  $R(t)$  and  $R_d(t)$  is given in terms of the attitude-error rotation matrix

$$\tilde{R} \triangleq R_d^T R \quad (35)$$

which satisfies the differential equation

$$\dot{\tilde{R}} = \tilde{R}\tilde{\omega}^\times \quad (36)$$

where the angular velocity error  $\tilde{\omega}$  is defined by

$$\tilde{\omega} \triangleq \omega - \tilde{R}^T \omega_d \quad (37)$$

Rewrite Eq. (19) in terms of  $\tilde{\omega}$  as

$$\begin{aligned} J_{sc} \dot{\tilde{\omega}} &= [J_{sc}(\tilde{\omega} + \tilde{R}^T \omega_d) + J_a \nu] \times (\tilde{\omega} + \tilde{R}^T \omega_d) \\ &+ J_{sc}(\tilde{\omega} \times \tilde{R}^T \omega_d - \tilde{R}^T \dot{\omega}_d) - J_a u + \tau_{dist} \end{aligned} \quad (38)$$

### A. Attitude Error

A scalar measure of attitude error is given by the eigenaxis attitude error, which is the rotation angle  $\theta(t)$  about the eigenaxis needed to rotate the spacecraft from its attitude  $R(t)$  to the desired attitude  $R_d(t)$ . This angle is given by [13]

$$\theta(t) = \cos^{-1} \left( \frac{1}{2} [\text{tr} \tilde{R}(t) - 1] \right) \quad (39)$$

### B. Spacecraft Inertia

Because the control laws in this paper require no inertia modeling, examples that span a range of possible inertia matrices are considered. The inertia of a rigid body is determined by its principal moments of inertia, that is, the diagonal entries of the inertia tensor resolved in a principal body-fixed frame, in which case the inertia matrix is a diagonal matrix. If the inertia tensor is resolved in a nonprincipal body-fixed frame, then the diagonal entries are the moments of inertia and the offdiagonal entries are the products of inertia. The offdiagonal entries of the inertia matrix are thus a consequence of an unknown rotation between a principal body-fixed frame and the chosen body-fixed frame.

Figure 1 shows the triangular region of feasible principal moments of inertia of a rigid body. There are five cases that are highlighted for the principal moments of inertia  $\lambda_1 \geq \lambda_2 \geq \lambda_3 > 0$ , where  $\lambda_1$ ,  $\lambda_2$ , and  $\lambda_3$  satisfy the triangle inequality  $\lambda_1 < \lambda_2 + \lambda_3$ . Let  $m$  denote the mass of the rigid body. The point  $\lambda_1 = \lambda_2 = \lambda_3$  corresponds to a sphere of radius  $r = \sqrt{\frac{5\lambda_1}{2m}}$ , a cube whose sides have length  $l = \sqrt{\frac{6\lambda_1}{m}}$ , and a cylinder of length  $l$  and radius  $r$ , in which  $l/r = \sqrt{3}$  and  $r = \sqrt{\frac{2\lambda_1}{m}}$ . The point  $\lambda_1 = \lambda_2 = 2\lambda_3$  corresponds to a cylinder of length  $l$  and radius  $r$ , in which  $l/r = 3$  and  $r = \sqrt{\frac{2\lambda_1}{m}}$ . The point  $\lambda_1 = \frac{6}{5}\lambda_2 = 2\lambda_3$ , located at the centroid of the triangular region, corresponds to a solid rectangular body with sides  $l_1 = \sqrt{\frac{8\lambda_1}{m}} > l_2 = \sqrt{\frac{4\lambda_1}{m}} > l_3 = \sqrt{\frac{2\lambda_1}{m}}$ .

The remaining cases in Fig. 1 are nonphysical, limiting cases. The point  $\lambda_1 = 2\lambda_2 = 2\lambda_3$  corresponds to a thin disk of radius  $r = \sqrt{\frac{2\lambda_1}{m}}$  and length  $l = 0$ . The point  $\lambda_1 = \lambda_2$  and  $\lambda_3 = 0$  corresponds to a thin cylinder of radius  $r = 0$  and length  $l = \sqrt{\frac{12\lambda_1}{m}}$ . Finally, each point along the line segment  $\lambda_1 = \lambda_2 + \lambda_3$ , in which  $\lambda_2 > \lambda_3$ , corresponds to a thin rectangular plate with sides of length  $l_1 = \sqrt{\frac{12\lambda_2}{m}} > l_2 = \sqrt{\frac{12\lambda_3}{m}}$ .

For all simulations of the inertia-free control laws, the principal axes are viewed as the nominal body-fixed axes, and thus, the nominal inertia matrix is a diagonal matrix whose diagonal entries are

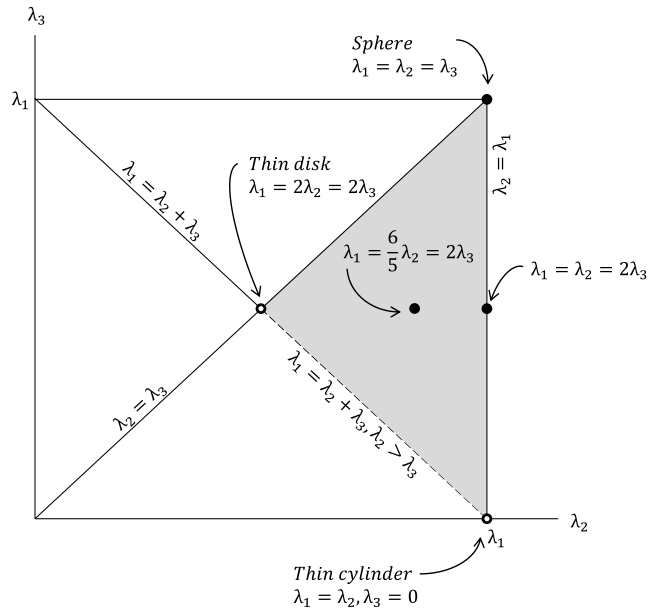


**Fig. 1** Feasible region of the principal moments of inertia  $\lambda_1$ ,  $\lambda_2$ , and  $\lambda_3$  of a rigid body satisfying  $0 < \lambda_3 \leq \lambda_2 \leq \lambda_1$ , where  $\lambda_1 < \lambda_2 + \lambda_3$ . The shaded region shows all feasible values of  $\lambda_2$  and  $\lambda_3$  in terms of the largest principal moment of inertia  $\lambda_1$ . The open dots and dashed line segment indicate nonphysical, limiting cases.

the principal moments of inertia. To demonstrate robustness, the principal moments as well as the orientation of the body-fixed frame relative to the principal axes are varied. For convenience,  $\lambda_1$  is normalized to  $10 \text{ kg} \cdot \text{m}^2$ , and the inertia matrices  $J_1, J_2, J_3, J_4$ , and  $J_5$  are chosen to correspond to the points noted in Fig. 1. These matrices, which correspond to the sphere, cylinder with  $l/r = 3$ , centroid, thin disk, and thin cylinder, respectively, are defined as

$$\begin{aligned} J_1 &= \text{diag}(10, 10, 10), & J_2 &= \text{diag}(10, 10, 5), \\ J_3 &= \text{diag}(10, 25/3, 5), & J_4 &= \text{diag}(10, 5, 5), \\ J_5 &= \text{diag}(10, 10, 0.1) \end{aligned} \quad (40)$$

The inertia matrix  $J_3$  corresponding to the centroid of the inertia region serves as the nominal inertia matrix, whereas the inertia matrices  $J_1, J_2, J_4$ , and  $J_5$  are used as perturbations to demonstrate robustness of the control laws. A perturbation  $J(\lambda)$  of  $J_i$  in the direction of  $J_j$  thus has the form

$$J(\lambda) = (1 - \lambda)J_i + \lambda J_j \quad (41)$$

where  $\lambda \in [0, 1]$ . Finally, in order to facilitate numerical integration of Euler's equation, note that  $J_5$  is chosen to be a nonsingular approximation of the limiting inertia of a thin cylinder.

## IV. Controller Design

Let  $I$  denote the identity matrix, for which the dimensions are determined by context, and let  $M_{ij}$  denote the  $i, j$  entry of the matrix  $M$ . The following result is given in [3].

**Lemma 1:** Let  $A \in \mathbb{R}^{3 \times 3}$  be a diagonal positive-definite matrix, and let  $R \in \mathbb{R}^{3 \times 3}$  be a rotation matrix. Then the following statements hold:

- 1) For all  $i, j = 1, 2, 3$ ,  $R_{ij} \in [-1, 1]$ .
- 2)  $\text{tr}(A - AR) \geq 0$ .
- 3)  $\text{tr}(A - AR) = 0$  if and only if  $R = I$ .

For convenience note that, if  $R$  is a rotation matrix and  $x, y \in \mathbb{R}^3$ , then

$$(Rx)^\times = Rx^\times R^T$$

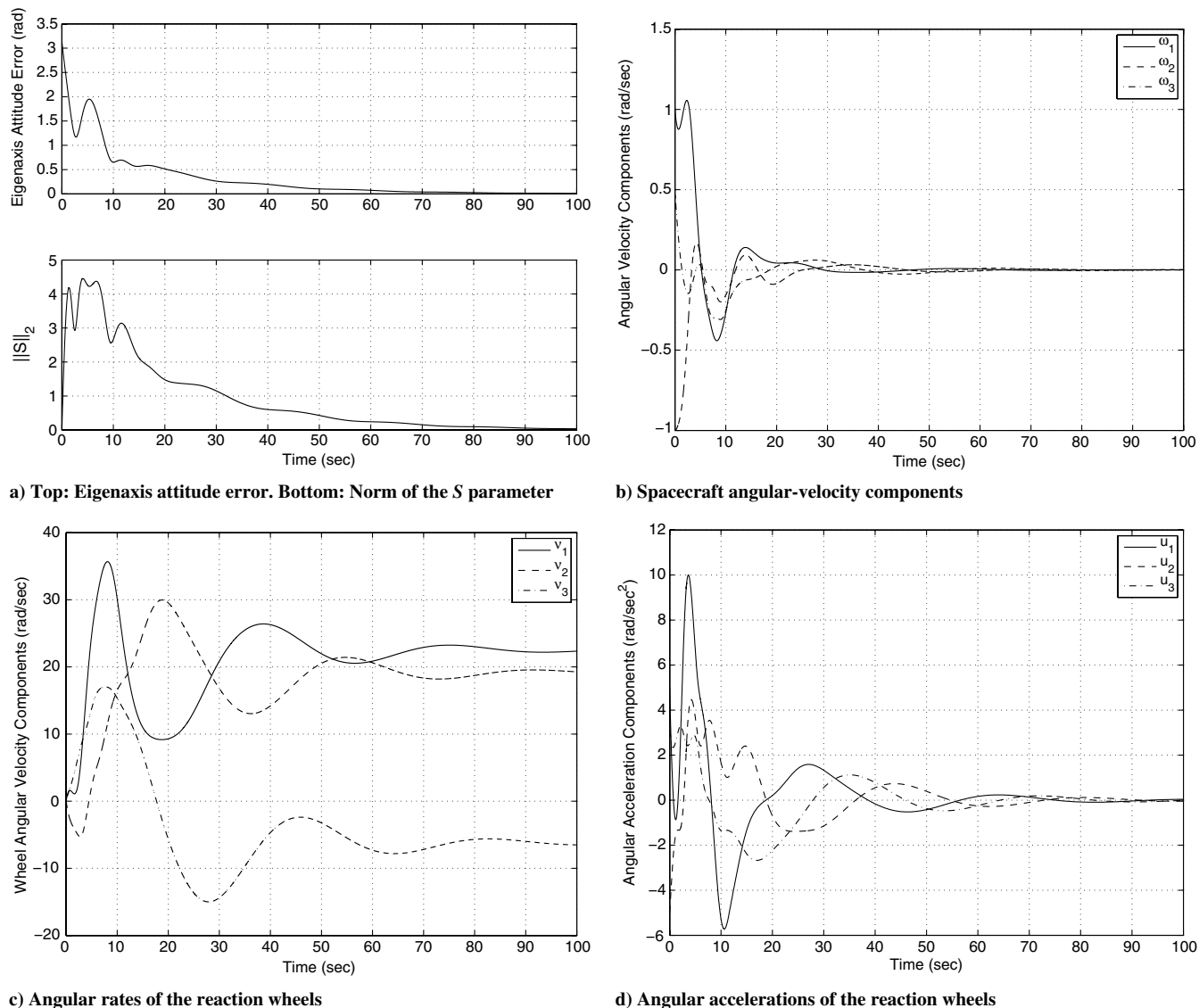


Fig. 2 Slewing maneuver using the control law (44) with no disturbance.

and therefore,

$$R(x \times y) = (Rx) \times Ry$$

Next, introduce the notation

$$J_{sc}\omega = L(\omega)\gamma$$

where  $\gamma \in \mathbb{R}^6$  is defined by

$$\gamma \triangleq [J_{11} \quad J_{22} \quad J_{33} \quad J_{23} \quad J_{13} \quad J_{12}]^T$$

and

$$L(\omega) \triangleq \begin{bmatrix} \omega_1 & 0 & 0 & 0 & \omega_3 & \omega_2 \\ 0 & \omega_2 & 0 & \omega_3 & 0 & \omega_1 \\ 0 & 0 & \omega_3 & \omega_2 & \omega_1 & 0 \end{bmatrix}$$

Next, let  $\hat{J}_{sc} \in \mathbb{R}^{3 \times 3}$  denote an estimate of  $J_{sc}$ , and define the inertia-estimation error:

$$\tilde{J}_{sc} \triangleq J_{sc} - \hat{J}_{sc}$$

Letting  $\hat{\gamma}, \tilde{\gamma} \in \mathbb{R}^6$  represent  $\hat{J}_{sc}, \tilde{J}_{sc}$ , respectively, it follows that

$$\tilde{\gamma} = \gamma - \hat{\gamma}$$

Likewise, let  $\hat{\tau}_{dist} \in \mathbb{R}^3$  denote an estimate of  $\tau_{dist}$ , and define the disturbance-estimation error:

$$\tilde{\tau}_{dist} \triangleq \tau_{dist} - \hat{\tau}_{dist}$$

The assumptions upon which the following development is based are now stated.

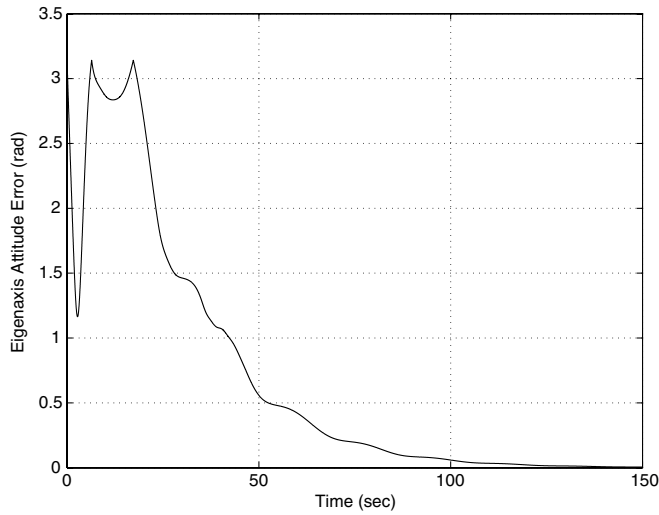
*Assumption 1:*  $J_{sc}$  is constant but unknown.

*Assumption 2:*  $J_a$  defined by Eq. (18) is constant, nonsingular, and known. That is, the spacecraft has three linearly independent, axisymmetric wheels with known moments of inertia about their spin axes and known configuration relative to the bus.

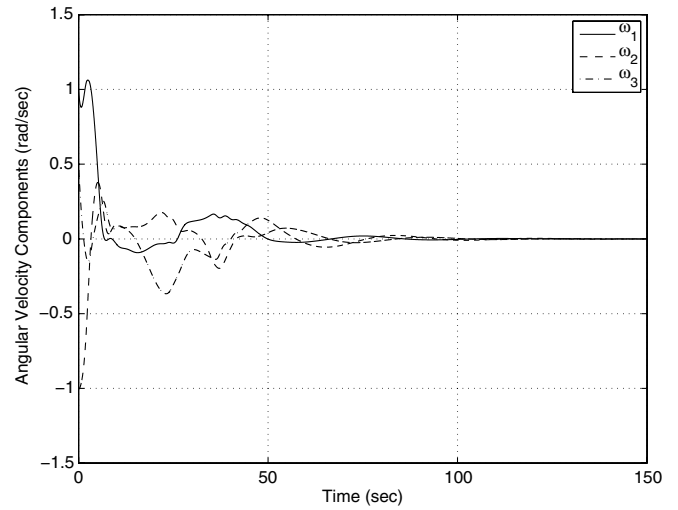
The controllers presented in [3] are now extended to the case of reaction-wheel actuation.

#### A. Control Law for Slewing Maneuvers

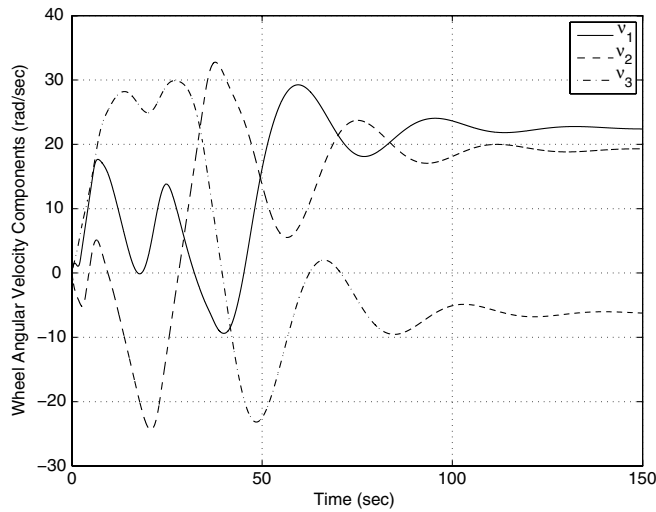
When no disturbances are present, the inertia-free control law given by Eq. (38) of [3] achieves almost global stabilization of a constant desired attitude  $R_d$ , that is, a slewing maneuver that brings the



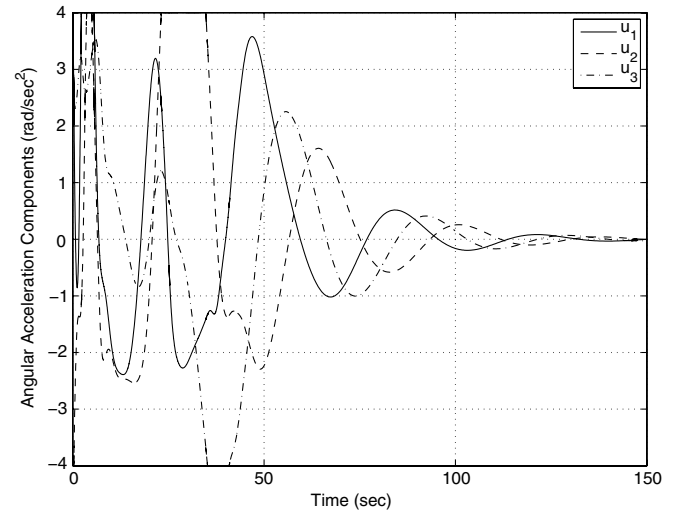
a) Eigenaxis attitude error



b) Spacecraft angular-velocity components



c) Angular rates of the reaction wheels



d) Angular accelerations of the reaction wheels

Fig. 3 Slew maneuver using the control law (44) with no disturbance. The acceleration of the reaction wheels is saturated at 4 rad/s<sup>2</sup>.

spacecraft to rest. The initial conditions of the slew maneuver may be arbitrary; that is, the spacecraft may have nonzero initial velocity.

Given  $a_1, a_2, a_3 \in \mathbb{R}$ , define the vector measure of attitude error:

$$S \triangleq \sum_{i=1}^3 a_i (\tilde{R}^T e_i) \times e_i \quad (42)$$

where, for  $i = 1, 2, 3$ ,  $e_i$  denotes the  $i$ th column of the  $3 \times 3$  identity matrix. When attitude measurements are given in terms of an alternative representation, such as quaternions, the corresponding attitude-error  $\tilde{R}$  defined by Eq. (35) can be computed, and thus, Eq. (42) can be evaluated and used by the controller given in Theorem 2 next. Consequently,  $S$  can be computed from any attitude parameterization.

*Theorem 1:* Let  $K_p$  be a positive number and let  $A = \text{diag}(a_1, a_2, a_3)$  be a diagonal positive-definite matrix. Then, the function

$$V(\omega, \tilde{R}) \triangleq \frac{1}{2} \omega^T J_{sc} \omega + K_p \text{tr}(A - A\tilde{R}) \quad (43)$$

is positive definite; that is,  $V$  is nonnegative, and  $V = 0$  if and only if  $\omega = 0$  and  $\tilde{R} = I$ .

*Proof:* It follows from statement 2 of Lemma 1 that  $\text{tr}(A - A\tilde{R})$  is nonnegative. Hence,  $V$  is nonnegative. Now, suppose that  $V = 0$ . Then,  $\omega = 0$ , and it follows from statement 3 of Lemma 1 that  $\tilde{R} = I$ .

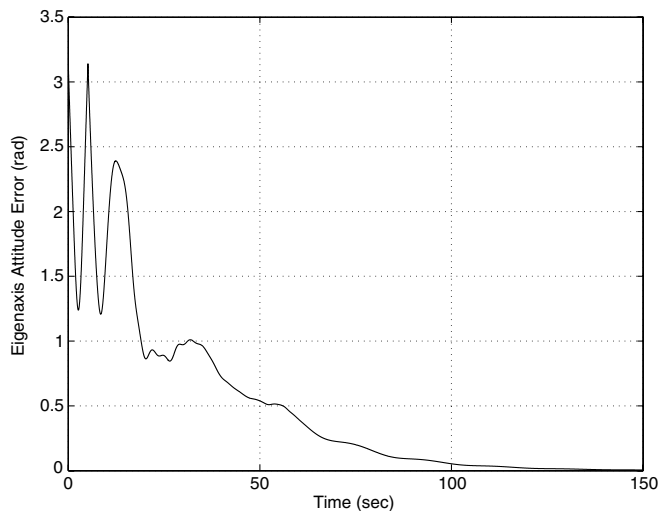
*Theorem 2:* Let  $K_p$  be a positive number, let  $K_v \in \mathbb{R}^{3 \times 3}$  be a positive-definite matrix, let  $A = \text{diag}(a_1, a_2, a_3)$  be a diagonal positive-definite matrix with distinct diagonal entries, let  $R_d$  be constant, define  $S$  as in Eq. (42), and define  $V$  as in Theorem 1. Consider the control law

$$u = J_a^{-1}(K_p S + K_v \omega) \quad (44)$$

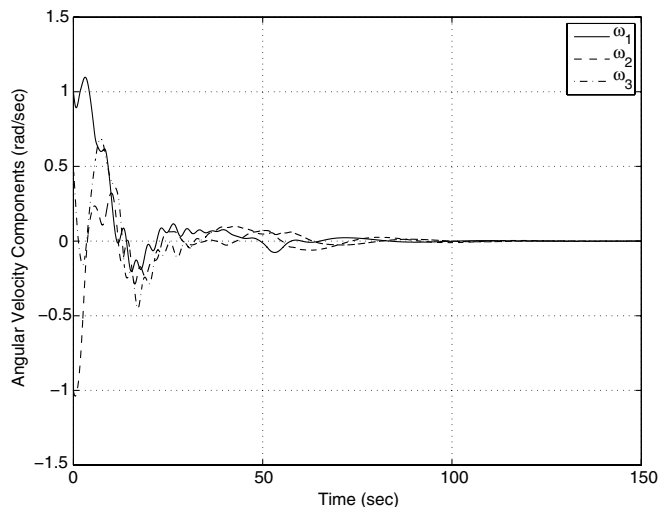
Then,

$$\dot{V}(\omega, \tilde{R}) = -\omega^T K_v \omega \quad (45)$$

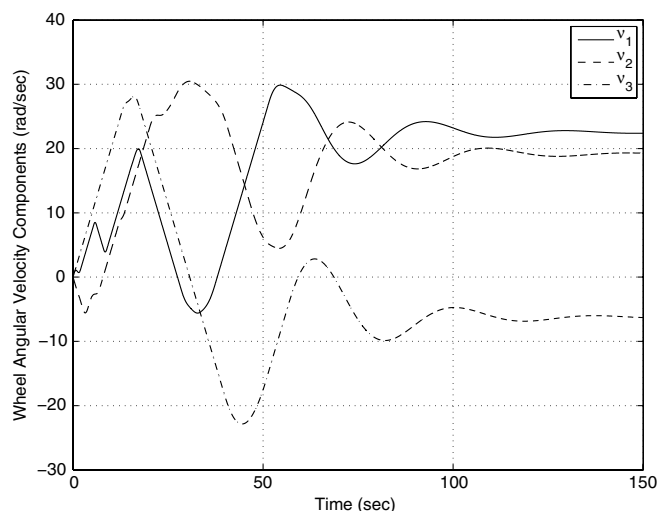
is negative semidefinite. Furthermore, the closed-loop system consisting of Eqs. (19), (20), (36), and (44) is almost globally asymptotically stable [14], and for all initial conditions not in an embedded submanifold of  $\mathbb{R}^3 \times \text{SO}(3) \times \mathbb{R}^6 \times \mathbb{R}^3$  (see [3]),  $\omega \rightarrow 0$  and  $\tilde{R} \rightarrow I$  as  $t \rightarrow \infty$ .



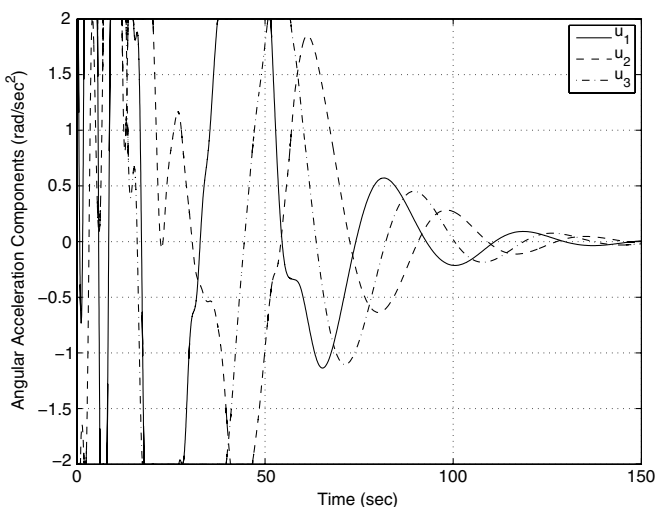
a) Eigenaxis attitude error



b) Spacecraft angular-velocity components



c) Angular rates of the reaction wheels



d) Angular accelerations of the reaction wheels

Fig. 4 Slew maneuver using the control law (44) with no disturbance. The acceleration of the reaction wheels is saturated at 2 rad/s<sup>2</sup>.

*Proof:* Noting that

$$\begin{aligned}
 & \frac{d}{dt} \text{tr}(A - A\tilde{R}) = -\text{tr}A\dot{\tilde{R}} \\
 & = -\text{tr}(A(\tilde{R}\omega^\times - \omega_d^\times \tilde{R})) \\
 & = -\sum_{i=1}^3 a_i e_i^T (\tilde{R}\omega^\times - \omega_d^\times \tilde{R}) e_i \\
 & = -\sum_{i=1}^3 a_i e_i^T \tilde{R}(\omega^\times - \tilde{R}^T \omega_d^\times \tilde{R}) e_i \\
 & = -\sum_{i=1}^3 a_i e_i^T \tilde{R}(\omega - \tilde{R}^T \omega_d)^\times e_i \\
 & = \sum_{i=1}^3 a_i e_i^T \tilde{R} e_i^\times \tilde{\omega} \\
 & = \left[ -\sum_{i=1}^3 a_i e_i \times \tilde{R}^T e_i \right]^T \tilde{\omega} \\
 & = \left[ \sum_{i=1}^3 a_i (\tilde{R}^T e_i) \times e_i \right]^T \tilde{\omega} \\
 & = \tilde{\omega}^T S
 \end{aligned}$$

then

$$\begin{aligned}
 \dot{V}(\omega, \tilde{R}) & = \omega^T J_{sc} \dot{\omega} + K_p \omega^T S \\
 & = \omega^T [(J_{sc} \omega + J_a \nu) \times \omega - J_a u] + K_p \omega^T S \\
 & = \omega^T (-K_p S - K_v \omega) + K_p \omega^T S \\
 & = -\omega^T K_v \omega
 \end{aligned}$$

The proof of the final statement follows from invariant set arguments that are similar to those used in [3].

Note that  $-J_a$  is substituted for the input matrix  $B$  used in the inertia-free control law (38) of [3], but otherwise, the controller requires no modification for the case of reaction-wheel actuation in order to achieve almost global stabilization of a constant desired attitude  $R_d$ .

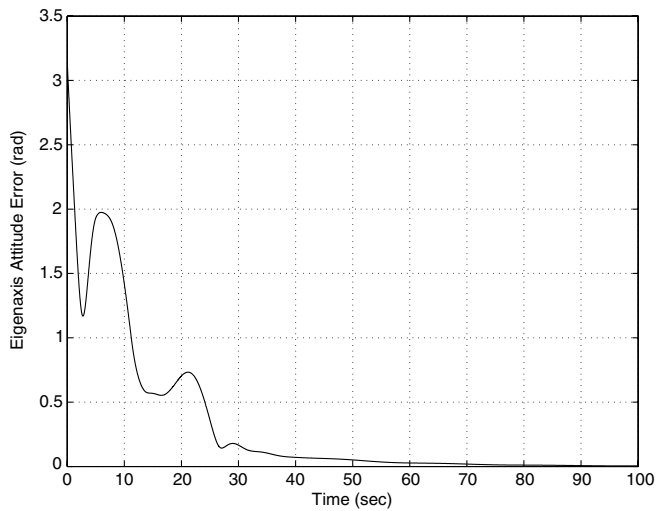
## B. Control Law for Attitude Tracking

A control law that tracks a desired attitude trajectory in the presence of disturbances is given by Eq. (21) of [3]. This controller is based on an additional assumption.

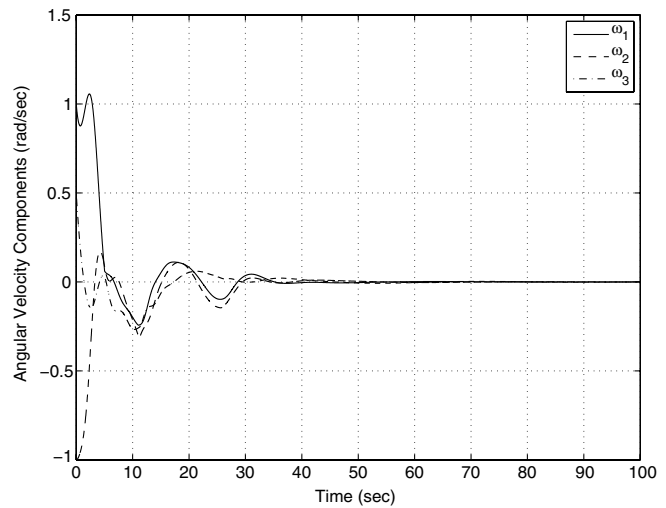
*Assumption 3:* Each component of  $\tau_{\text{dist}}$  is a linear combination of constant and harmonic signals, for which the frequencies are known but for which the amplitudes and phases are unknown.

Assumption 3 implies that  $\tau_{\text{dist}}$  can be modeled as the output of the autonomous system

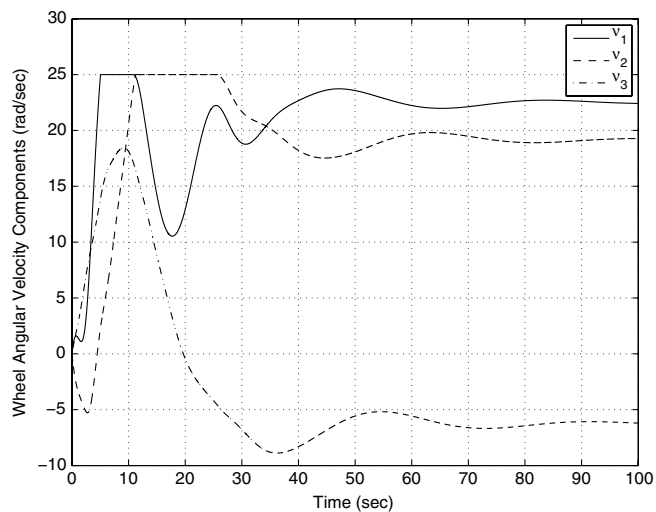
$$\dot{d} = A_d d \quad (46)$$



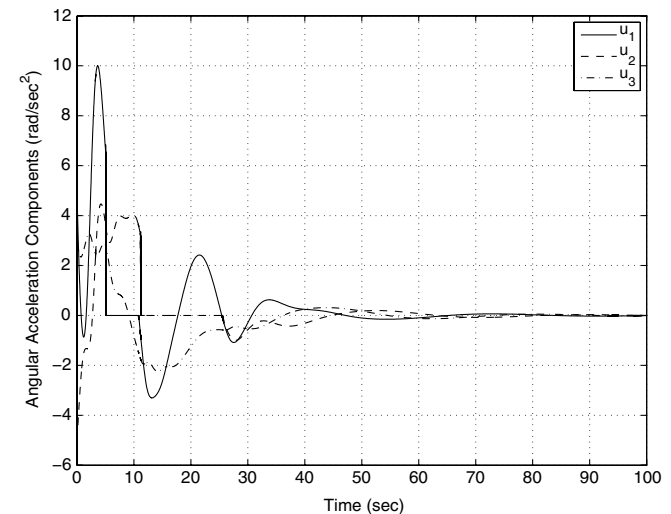
a) Eigenaxis attitude error



b) Spacecraft angular-velocity components



c) Angular rates of the reaction wheels



d) Angular accelerations of the reaction wheels

Fig. 5 Slew maneuver using the control law (44) with no disturbance. The maximum rotation rate of each wheel is saturated at 25 rad/s.

$$\tau_{\text{dist}} = C_d d \quad (47)$$

where  $d$  is the disturbance state,  $A_d \in \mathbb{R}^{n_d \times n_d}$  and  $C_d \in \mathbb{R}^{3 \times n_d}$  are known matrices, and the eigenvalues of  $A_d$  are nonrepeated on the imaginary axis. In this model,  $d(0)$  is unknown, which is equivalent to the assumption that the amplitude and phase of each harmonic component of the disturbance is unknown. The eigenvalues of  $A_d$  are chosen to represent all frequency components that may be present in the disturbance signal, in which the zero eigenvalue corresponds to a constant disturbance. By providing infinite gain at the disturbance frequencies, the controller asymptotically rejects the harmonic disturbances. In particular, an integral controller provides infinite gain at zero frequency in order to reject constant disturbances. In the case of orbit-dependent disturbances, the frequencies can be estimated from the orbital parameters. Likewise, in the case of disturbances originating from onboard devices, the spectral content of the disturbances may be known. In other cases, it may be possible to estimate the spectrum of the disturbances through signal processing. Assumption 3 implies that  $A_d$  can be chosen to be skew symmetric, which is henceforth done. Let  $\hat{d} \in \mathbb{R}^{n_d}$  denote an estimate of  $d$ , and define the disturbance-state estimation error:

$$\tilde{d} \triangleq d - \hat{d}$$

The attitude tracking controller in the presence of disturbances given in [3] is modified next for reaction-wheel actuators.

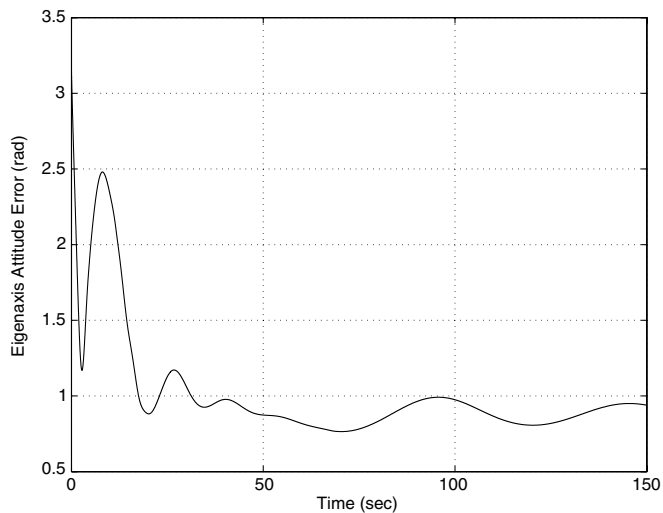
*Theorem 3:* Let  $K_p$  be a positive number, let  $K_1 \in \mathbb{R}^{3 \times 3}$ , let  $Q \in \mathbb{R}^{6 \times 6}$  and  $D \in \mathbb{R}^{n_d \times n_d}$  be positive-definite matrices, let  $A = \text{diag}(a_1, a_2, a_3)$  be a diagonal positive-definite matrix, and define  $S$  as in Eq. (42). Then, the function

$$V(\tilde{\omega}, \tilde{R}, \tilde{\gamma}, \tilde{d}) \triangleq \frac{1}{2} (\tilde{\omega} + K_1 S)^T J_{\text{sc}} (\tilde{\omega} + K_1 S) + K_p \text{tr}(A - A\tilde{R}) + \frac{1}{2} \tilde{\gamma}^T Q \tilde{\gamma} + \frac{1}{2} \tilde{d}^T D \tilde{d} \quad (48)$$

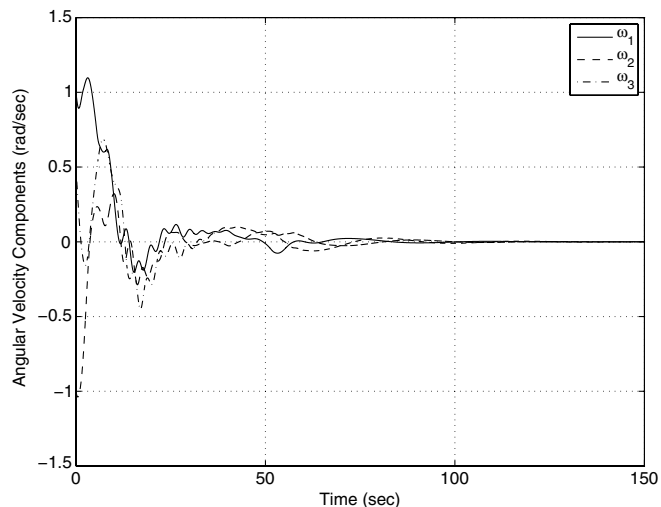
is positive definite; that is,  $V$  is nonnegative, and  $V = 0$  if and only if  $\tilde{\omega} = 0$ ,  $\tilde{R} = I$ ,  $\tilde{\gamma} = 0$ , and  $\tilde{d} = 0$ .

*Proof:* It follows from statement 2 of Lemma 1 that  $\text{tr}(A - A\tilde{R})$  is nonnegative. Hence,  $V$  is nonnegative. Now, suppose that  $V = 0$ . Then,  $\tilde{\omega} + K_1 S = 0$ ,  $\tilde{\gamma} = 0$ , and  $\tilde{d} = 0$ , and it follows from statement 3 of Lemma 1 that  $\tilde{R} = I$ , and thus,  $S = 0$ . Therefore,  $\tilde{\omega} = 0$ .

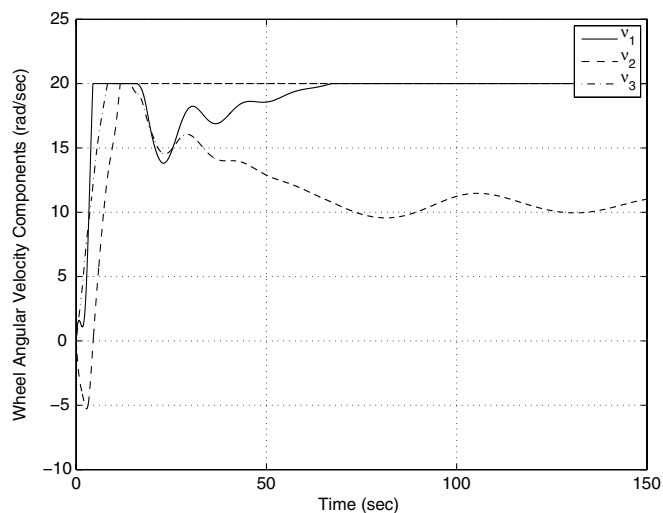
The following result concerns attitude tracking without knowledge of the spacecraft inertia. This control law does not regulate the speed of the wheels. Consequently, the function  $V$  defined by Eq. (48), which is used as a Lyapunov function in the proof of Theorem 4 next, is not a positive-definite function of the angular rates of the wheels relative to the bus.



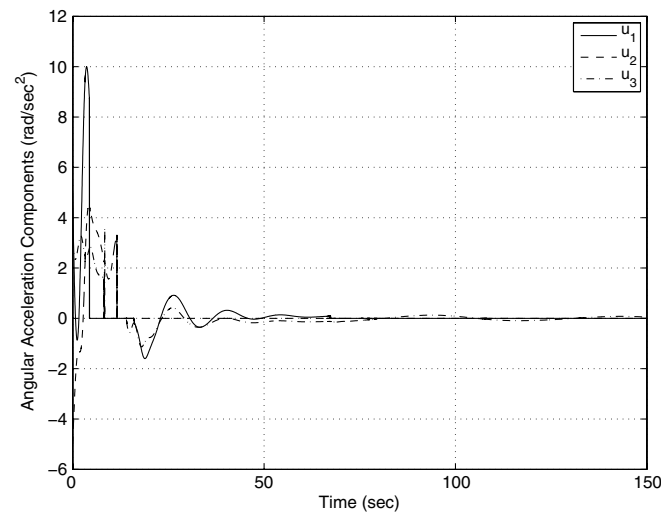
a) Eigenaxis attitude error



b) Spacecraft angular-velocity components



c) Angular rates of the reaction wheels



d) Angular accelerations of the reaction wheels

**Fig. 6** Slew maneuver using the control law (44) with no disturbance. The maximum rotation rate of each wheel is saturated at 20 rad/s.

*Theorem 4:* Let  $K_p$  be a positive number, let  $K_v \in \mathbb{R}^{3 \times 3}$ ,  $K_1 \in \mathbb{R}^{3 \times 3}$ ,  $Q \in \mathbb{R}^{6 \times 6}$ , and  $D \in \mathbb{R}^{n_d \times n_d}$  be positive-definite matrices, assume that  $A_d^T D + D A_d$  is negative semidefinite, let  $A = \text{diag}(a_1, a_2, a_3)$  be a diagonal positive-definite matrix with distinct diagonal entries, define  $S$  and  $V$  as in Theorem 3, and let  $\hat{\gamma}$  and  $\hat{d}$  satisfy

$$\dot{\hat{\gamma}} = Q^{-1}[L^T(\omega)\omega^\times + L^T(K_1\dot{S} + \tilde{\omega} \times \omega - \tilde{R}^T\dot{\omega}_d)](\tilde{\omega} + K_1S) \quad (49)$$

where

$$\dot{S} = \sum_{i=1}^3 a_i [(\tilde{R}^T e_i) \times \tilde{\omega}] \times e_i \quad (50)$$

and

$$\hat{d} = A_d \hat{d} + D^{-1} C_d^T (\tilde{\omega} + K_1 S) \quad (51)$$

$$\hat{\tau}_{\text{dist}} = C_d \hat{d} \quad (52)$$

so that  $\hat{\tau}_{\text{dist}}$  is the disturbance-torque estimate. Consider the control law

$$u = -J_\alpha^{-1}(v_1 + v_2 + v_3) \quad (53)$$

where

$$v_1 \triangleq -(\hat{J}_{\text{sc}}\omega + J_\alpha v) \times \omega - \hat{J}_{\text{sc}}(K_1\dot{S} + \tilde{\omega} \times \omega - \tilde{R}^T\dot{\omega}_d) \quad (54)$$

$$v_2 \triangleq -\hat{\tau}_{\text{dist}} \quad (55)$$

and

$$v_3 \triangleq -K_v(\tilde{\omega} + K_1 S) - K_p S \quad (56)$$

Then,

$$\begin{aligned} \dot{V}(\tilde{\omega}, \tilde{R}, \tilde{\gamma}, \tilde{d}) &= -(\tilde{\omega} + K_1 S)^T K_v (\tilde{\omega} + K_1 S) - K_p S^T K_1 S \\ &\quad + \frac{1}{2} \tilde{d}^T (A_d^T D + D A_d) \tilde{d} \end{aligned} \quad (57)$$

is negative semidefinite. Furthermore, the closed-loop system consisting of Eqs. (20), (36), (38), and (53) is almost globally asymptotically stable, and for all initial conditions not in an embedded submanifold of  $\mathbb{R}^3 \times SO(3) \times \mathbb{R}^6 \times \mathbb{R}^3$  (see [3]),  $\tilde{\omega} \rightarrow 0$  and  $\tilde{R} \rightarrow I$  as  $t \rightarrow \infty$ .

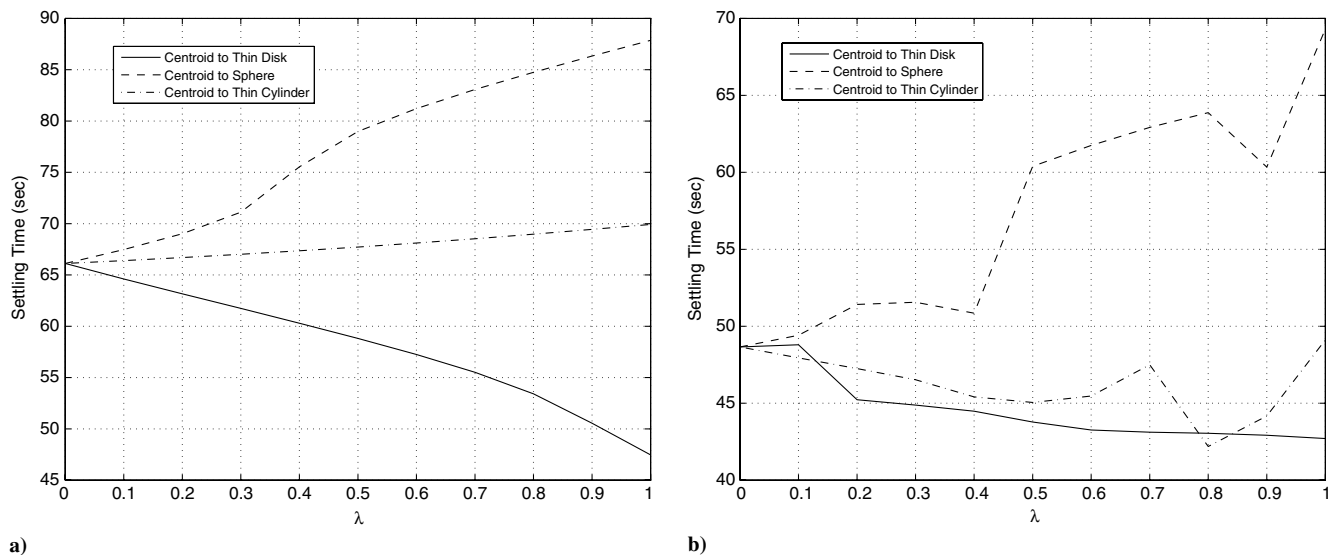


Fig. 7 Settling time as a function of  $\lambda$  for various combinations (41) of inertia matrices resolved in principal frames. Convergence is achieved for a) control law (44) and b) control law (53). Each controller is implemented in all cases with a single tuning. In all cases, the bus inertia  $J_3$  is unknown.

Proof:

$$\begin{aligned}
 \dot{V}(\tilde{\omega}, \tilde{R}, \tilde{\gamma}, \tilde{d}) &= (\tilde{\omega} + K_1 S)^T (J_{sc} \dot{\tilde{\omega}} + J_{sc} K_1 \dot{S}) - K_p \text{tr} A \tilde{R} - \tilde{\gamma}^T Q \dot{\tilde{\gamma}} \\
 &+ \tilde{d}^T D \dot{\tilde{d}} = (\tilde{\omega} + K_1 S)^T [(J_{sc} \omega + J_{\alpha} \nu) \times \omega \\
 &+ J_{sc} (\tilde{\omega} \times \omega - \tilde{R}^T \dot{\omega}_d) - J_{\alpha} u + \tau_{\text{dist}} + J_{sc} K_1 \dot{S}] \\
 &+ K_p \tilde{\omega}^T S - \tilde{\gamma}^T Q \dot{\tilde{\gamma}} + \tilde{d}^T D \dot{\tilde{d}} \\
 &= (\tilde{\omega} + K_1 S)^T [(J_{sc} \omega + J_{\alpha} \nu) \times \omega \\
 &+ J_{sc} (K_1 \dot{S} + \tilde{\omega} \times \omega - \tilde{R}^T \dot{\omega}_d) \\
 &+ v_1 + v_2 + v_3 + \tau_{\text{dist}}] + K_p \tilde{\omega}^T S - \tilde{\gamma}^T Q \dot{\tilde{\gamma}} + \tilde{d}^T D \dot{\tilde{d}} \\
 &= (\tilde{\omega} + K_1 S)^T [(\tilde{J}_{sc} \omega) \times \omega + \tilde{J}_{sc} (K_1 \dot{S} + \tilde{\omega} \times \omega - \tilde{R}^T \dot{\omega}_d)] \\
 &+ (\tilde{\omega} + K_1 S)^T \tilde{\tau}_{\text{dist}} - (\tilde{\omega} + K_1 S)^T K_v (\tilde{\omega} + K_1 S) \\
 &- K_p (\tilde{\omega} + K_1 S)^T S + K_p \tilde{\omega}^T S - \tilde{\gamma}^T Q \dot{\tilde{\gamma}} + \tilde{d}^T D \dot{\tilde{d}} \\
 &= (\tilde{\omega} + K_1 S)^T [L(\omega) \tilde{\gamma} \times \omega + L(K_1 \dot{S} + \tilde{\omega} \times \omega - \tilde{R}^T \dot{\omega}_d) \tilde{\gamma}] \\
 &- (\tilde{\omega} + K_1 S)^T K_v (\tilde{\omega} + K_1 S) - K_p S^T K_1 S - \tilde{\gamma}^T Q \dot{\tilde{\gamma}} \\
 &+ \tilde{d}^T C_d^T (\tilde{\omega} + K_1 S) + \tilde{d}^T D [A_d \tilde{d} - D^{-1} C_d^T (\tilde{\omega} + K_1 S)] \\
 &= -(\tilde{\omega} + K_1 S)^T K_v (\tilde{\omega} + K_1 S) - K_p S^T K_1 S - \tilde{\gamma}^T Q \dot{\tilde{\gamma}} \\
 &+ (\tilde{\omega} + K_1 S)^T [-\omega \times L(\omega) + L(K_1 \dot{S} + \tilde{\omega} \times \omega - \tilde{R}^T \dot{\omega}_d)] \tilde{\gamma} \\
 &+ \frac{1}{2} \tilde{d}^T (A_d^T D + D A_d) \tilde{d} \\
 &= -(\tilde{\omega} + K_1 S)^T K_v (\tilde{\omega} + K_1 S) - K_p S^T K_1 S \\
 &+ \tilde{\gamma}^T [-Q \dot{\tilde{\gamma}} + (L^T(\omega) \omega \times + L^T(K_1 \dot{S} + \tilde{\omega} \times \omega \\
 &- \tilde{R}^T \dot{\omega}_d)) (\tilde{\omega} + K_1 S)] + \frac{1}{2} \tilde{d}^T (A_d^T D + D A_d) \tilde{d} \\
 &= -(\tilde{\omega} + K_1 S)^T K_v (\tilde{\omega} + K_1 S) - K_p S^T K_1 S \\
 &+ \frac{1}{2} \tilde{d}^T (A_d^T D + D A_d) \tilde{d}
 \end{aligned}$$

$$\begin{aligned}
 J \dot{\tilde{\omega}} &= [L(\omega) \tilde{\gamma}] \times \omega + L(\tilde{\omega} \times \tilde{R}^T \omega_d - R^T \dot{\omega}_d) \tilde{\gamma} - L(K_1 \dot{S}) \dot{\tilde{\gamma}} \\
 &+ \tilde{z}_d - K_v (\tilde{\omega} + K_1 S) - K_p S
 \end{aligned} \quad (58)$$

From Lemmas 3 and 4 of [3], the closed-loop system consisting of Eqs. (49–52) and (58) has four disjoint equilibrium manifolds. These equilibrium manifolds in  $\mathbb{R}^3 \times \text{SO}(3) \times \mathbb{R}^6 \times \mathbb{R}^3$  are given by

$$\begin{aligned}
 \mathcal{E}_i &= \{(\tilde{\omega}, \tilde{R}, \tilde{\gamma}, \tilde{d}) \in \mathbb{R}^3 \times \text{SO}(3) \times \mathbb{R}^6 \\
 &\times \mathbb{R}^3 : \tilde{R} = \mathcal{R}_i, \tilde{\omega} \equiv 0, (\tilde{\gamma}, \tilde{d}) \in \mathcal{Q}_i\}
 \end{aligned} \quad (59)$$

where, for all  $i \in \{0, 1, 2, 3\}$ ,  $\mathcal{Q}_i$  is the closed subset of  $\mathbb{R}^6 \times \mathbb{R}^3$  defined by

$$\begin{aligned}
 \mathcal{Q}_i &\triangleq \{(\tilde{\gamma}, \tilde{d}) \in \mathbb{R}^6 \times \mathbb{R}^3 : [L(\mathcal{R}_i^T \omega_d) \tilde{\gamma}] \times (\mathcal{R}_i^T \omega_d) \\
 &= L(\mathcal{R}_i^T \omega_d) \tilde{\gamma} + C_d \tilde{d} = 0, \dot{\tilde{\gamma}} = 0, \dot{\tilde{d}} = A_d \tilde{d}\}
 \end{aligned}$$

Furthermore, the equilibrium manifold  $(\tilde{\omega}, \tilde{R}, (\tilde{\gamma}, \tilde{d})) = (0, I, \mathcal{Q}_0)$  of the closed-loop system given by Eqs. (49–52) and (58) is locally asymptotically stable, and the remaining equilibrium manifolds given by  $(0, \mathcal{R}_i, \mathcal{Q}_i)$  for  $i \in \{1, 2, 3\}$  are unstable. Finally, the set of all initial conditions converging to these equilibrium manifolds forms a lower-dimensional submanifold of  $\mathbb{R}^3 \times \text{SO}(3) \times \mathbb{R}^6 \times \mathbb{R}^3$ .

## V. Examples

Simulations are now provided to illustrate the inertia-free control laws (44) and (53). To simulate slew and spin maneuvers, the following spacecraft parameters are assumed. The bus inertia matrix  $J_b$  is nominally given by  $J_3$ , which corresponds to the centroid of the inertia region shown in Fig. 1 with the body-fixed frame assumed to be a principal body-fixed frame. The quantity  $J_b$  is unknown to the controller. The axes of rotation of the reaction wheels are aligned with the spacecraft body-fixed frame unit vectors, and the wheel inertias are given by  $J_{w_1} = \text{diag}(\alpha_1, \beta_1, \beta_1)$  kg  $\cdot$  m<sup>2</sup>,  $J_{w_2} = \text{diag}(\beta_2, \alpha_2, \beta_2)$  kg  $\cdot$  m<sup>2</sup>, and  $J_{w_3} = \text{diag}(\beta_3, \beta_3, \alpha_3)$  kg  $\cdot$  m<sup>2</sup>, where  $\alpha_1 = \alpha_2 = \alpha_3 = 0.5$  and  $\beta_1 = \beta_2 = \beta_3 = 0.375$ . The values of  $\beta_i$  are unknown to the controller.

Let  $K_p$  be given by

$$K_p = \frac{\gamma}{\text{tr} A} \quad (60)$$

The closed-loop spacecraft attitude dynamics Eq. (38) and the control law Eqs. (53–56) can be expressed as

and, as in [3], let  $K_v = K_v(\omega)$  be given by

$$K_v = \eta \begin{bmatrix} \frac{1}{1+|\omega_1|} & 0 & 0 \\ 0 & \frac{1}{1+|\omega_2|} & 0 \\ 0 & 0 & \frac{1}{1+|\omega_3|} \end{bmatrix} \quad (61)$$

Alternative choices of  $K_v$  are given in [15].

#### A. Slew Maneuver Using Control Law (44) with No Disturbance

Controller (44) is used for an aggressive slew maneuver, in which the objective is to bring the spacecraft from the initial attitude  $R_0 = I_3$  and initial angular velocity

$$\omega(0) = [1 \quad -1 \quad 0.5]^T \text{ rad/s}$$

to rest ( $\omega_d = 0$ ) at the desired final orientation  $R_d = \text{diag}(1, -1, -1)$ , which represents a rotation of 180 deg about the  $x$  axis. The reaction wheels are initially not spinning relative to the spacecraft; that is,

$$v(0) = [0 \quad 0 \quad 0]^T \text{ rad/s}$$

No disturbance is present, and the parameters  $\gamma = \eta = 5$  are used in Eqs. (60) and (61).

Figures 2a–2d show, respectively, the attitude error, angular-velocity components, angular rates of the wheels, and the control inputs, which are the angular accelerations of the wheels. The spacecraft attitude and angular-velocity components reach the commanded values in about 100 s. The angular rates of the wheels approach constant values that are consistent with the initial, nonzero angular momentum.

In practice, reaction wheels have a maximum instantaneous acceleration. Angular-acceleration saturation is enforced in Figs. 3 and 4, in which convergence is slower than in Fig. 2, although stability is maintained.

Additionally, reaction wheels have a maximum rotational rate. Figure 5 shows the effect of wheel-rate saturation at 25 rad/s, corresponding to about 240 rpm. The reaction-wheel rates are saturated for up to 25 s, although this does not impact the control objective. Figure 6 shows plots for wheel-rate saturation at 20 rad/s or about 190 rpm. Although this constraint on the rotation rate is too stringent to obtain zero steady-state error for the desired maneuver, the performance of the controller degrades

gracefully by achieving zero spacecraft angular velocity at an offset attitude.

To evaluate performance for slew maneuvers, define the settling-time metric

$$k_0 \triangleq \min_{k > 100} \{k : \text{for all } i \in \{1, \dots, 100\}, \theta((k-i)T_s) < 0.05 \text{ rad}\} \quad (62)$$

where  $k$  is the simulation step,  $T_s$  is the integration step size, and  $\theta(kT_s)$  is the eigenaxis attitude error (39) at the  $k$ th simulation step. The metric  $k_0$  is thus the minimum time such that the eigenaxis attitude error is less than 0.05 rad during the 100 most recent simulation steps.

To illustrate the inertia-free property of the control laws (44) and (53), the inertia of the spacecraft is varied using

$$J_b(\lambda) = (1 - \lambda)J_3 + \lambda J_i \quad (63)$$

where  $\lambda \in [0, 1]$  and  $i = 1, 4, 5$ . Figure 7 shows how the settling time depends on  $\lambda$ .

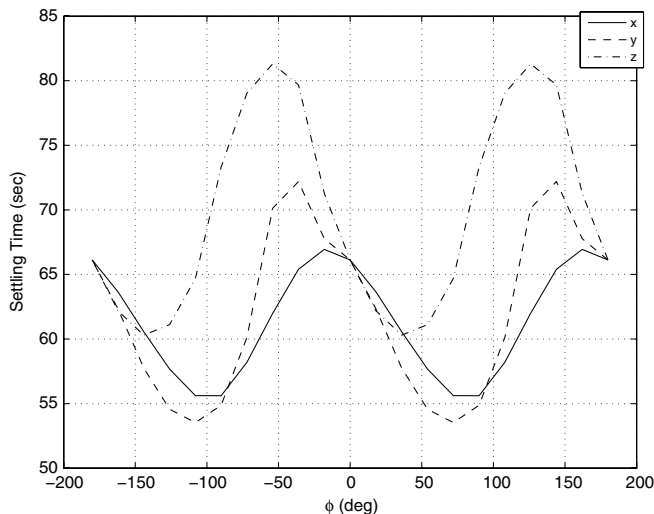
Next, the robustness to misalignment of the reaction wheels relative to the principal axes is investigated. Here, the inertia matrix is rotated by an angle  $\phi$  about one of the axes of frame  $F_b$ . For a rotation about the  $x$  axis of  $F_b$ , the inertia of the spacecraft is varied using

$$J_b(\phi) = \mathcal{O}_1(\phi)J_3\mathcal{O}_1^T(\phi) \quad (64)$$

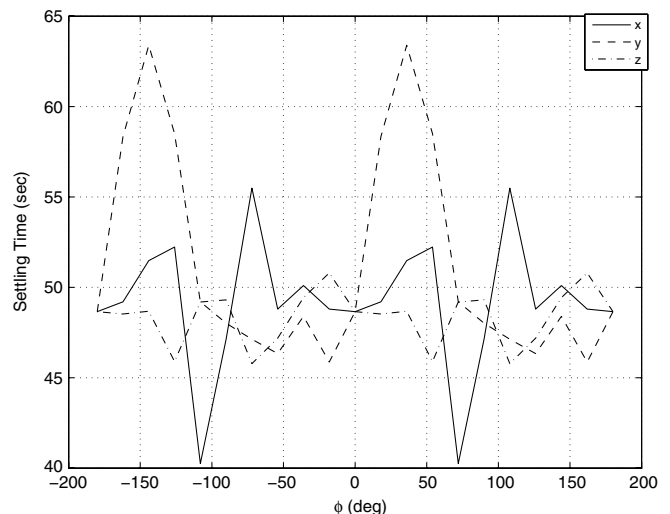
where the proper orthogonal matrix  $\mathcal{O}_1(\phi)$  rotates vectors about the  $x$  axis by the angle  $\phi$ . Similar relations exist for rotations about the  $y$  and  $z$  axes. Figure 8 shows how a thruster misalignment angle  $\phi$  affects the settling time, in which  $\phi$  is varied from  $-180$  to  $+180$  deg.

#### B. Slew Maneuver Using Control Law (53) Under Constant Disturbance

The unknown constant disturbance torque  $\tau_{\text{dist}} = [0.7 \quad -0.30]^T$  is now considered. Note that the controller (53) is used in place of the controller (44), which lacks an integrator, and thus has a constant steady-state error bias due to the persistent disturbance. The parameters of the controller (53) are chosen to be  $K_1 = I_3$ ,  $A = \text{diag}(1, 2, 3)$ ,  $\gamma = \eta = 1$ ,  $D = I_3$ , and  $Q = I_6$ .

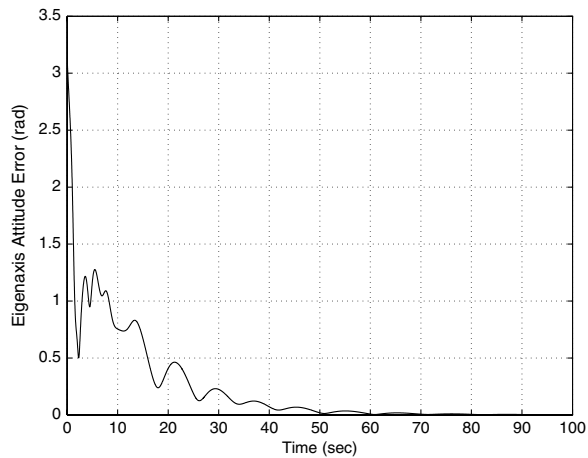


a)

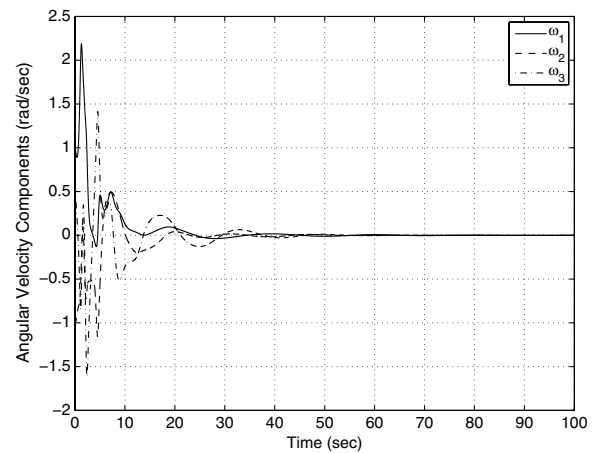


b)

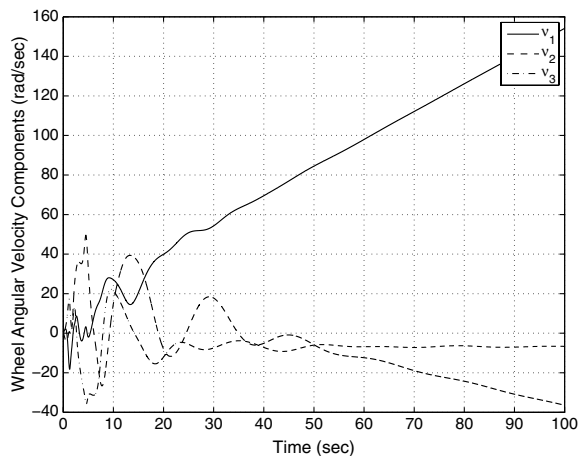
**Fig. 8** Settling time as a function of principal-frame/body-frame rotation angle  $\phi$  for rotations about each of the three principal axes of  $J_3$ . Convergence is achieved for a) control law (44) and b) control law (53).



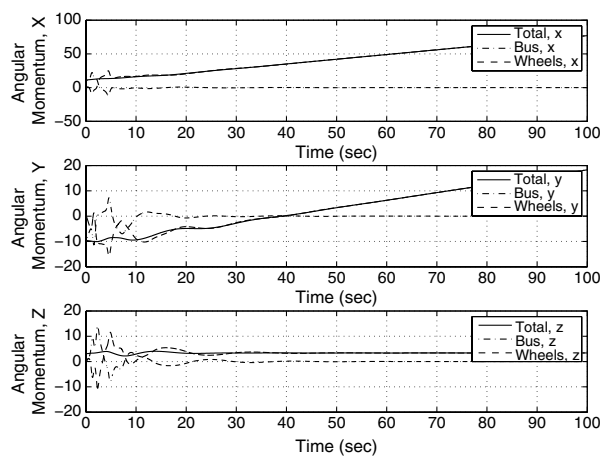
a) Eigenaxis attitude error



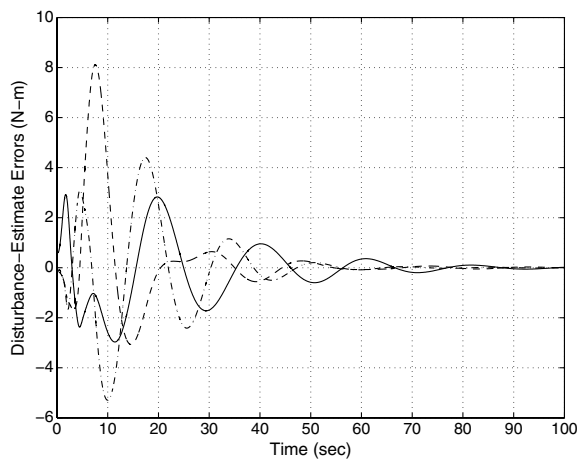
b) Spacecraft angular-velocity components



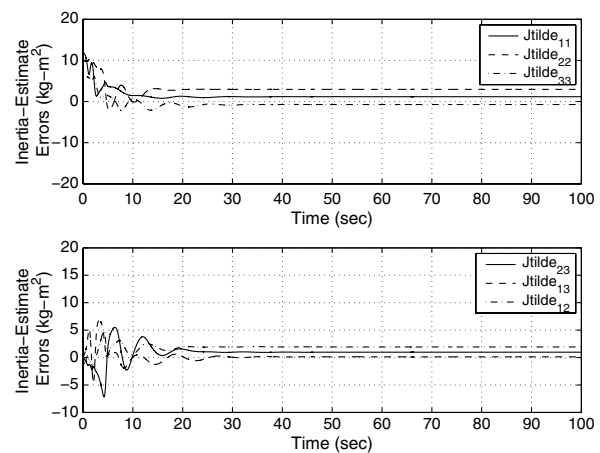
c) Angular rates of the reaction wheels. The spin rate grows unbounded due to the constant disturbance torque



d) Angular momentum of the spacecraft relative to its center of mass with respect to the inertial frame resolved in the inertial frame. The total angular momentum is not conserved due to the constant disturbance torque in the bus-fixed frame



e) Disturbance-estimate errors



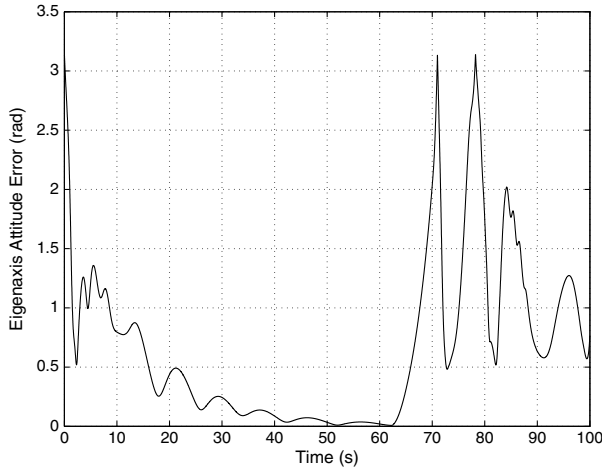
f) Inertia-estimate errors

**Fig. 9** Slew maneuver using the control law (53) under a disturbance that is constant with respect to the bus-fixed frame.

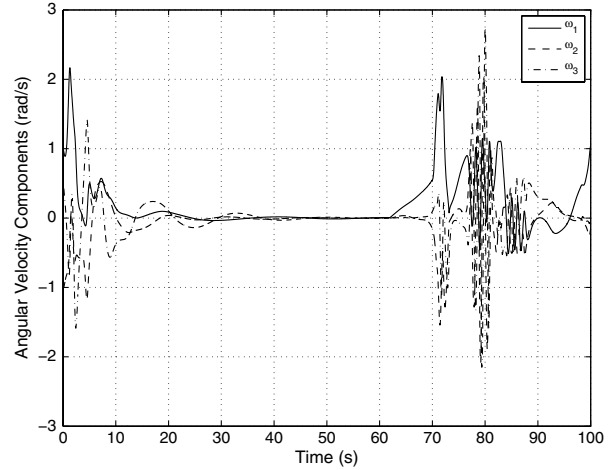
Figures 9a–9f show, respectively, the attitude error, angular velocity components, angular rates of the wheels, angular momentum, disturbance-estimate errors, and inertia-estimate errors. The spacecraft attitude and angular velocity components reach the commanded values in about 80 s. Figure 9c indicates that the reaction-wheel rotational speed grows unbounded. Figure 9d shows that the total angular momentum of the spacecraft increases, which is consistent

with the constant disturbance torque acting on the spacecraft. In practice, the spacecraft needs a method to dump the stored angular momentum so that the reaction wheel rates do not grow unbounded.

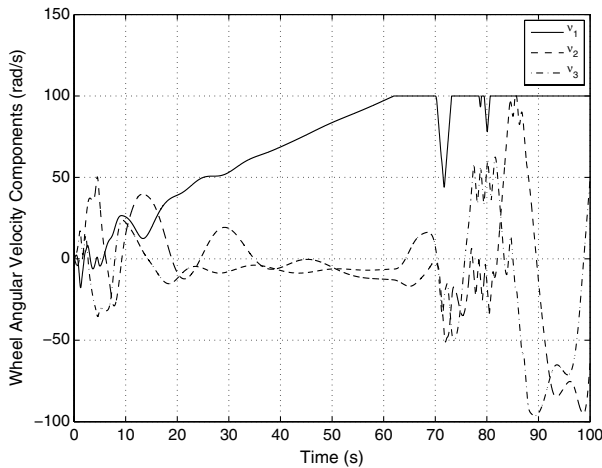
Figure 10 repeats the maneuver with maximum wheel saturation at 100 rad/s, corresponding to roughly 1000 rpm. The controller brings the spacecraft to the desired orientation in about 60 s at which time one of the angular rates of the reaction wheels reaches



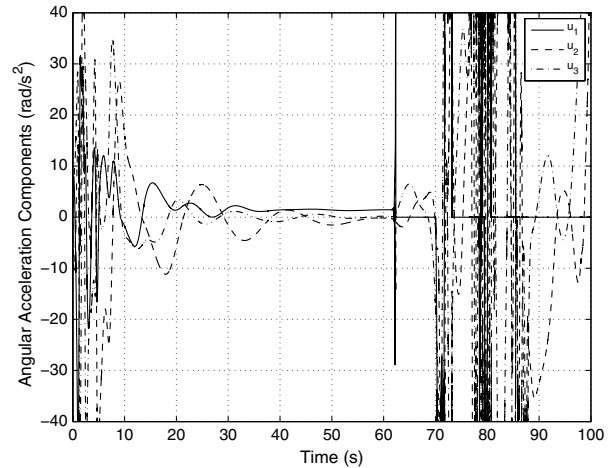
a) Eigen axis attitude error



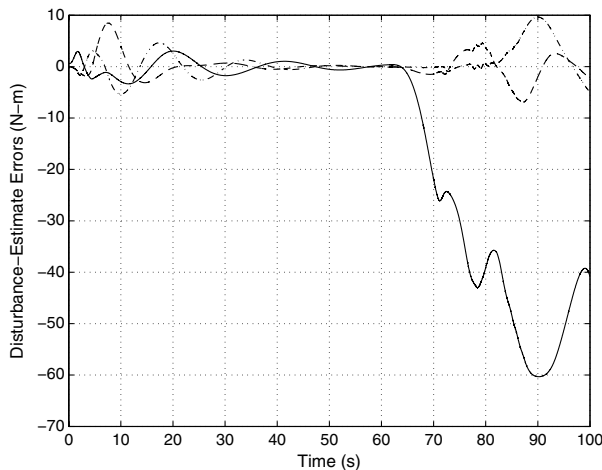
b) Spacecraft angular-velocity components



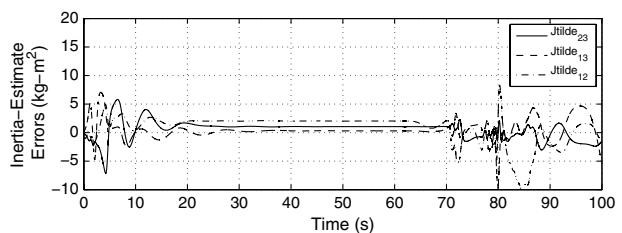
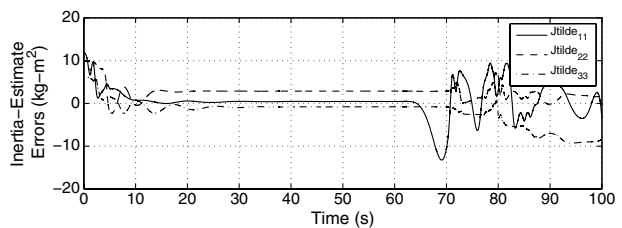
c) Angular rates of the reaction wheels. The spin rate grows until reaching the saturation limit of 100 rad/s



d) Angular accelerations of the reaction wheels



e) Disturbance-estimate errors



f) Inertia-estimate errors

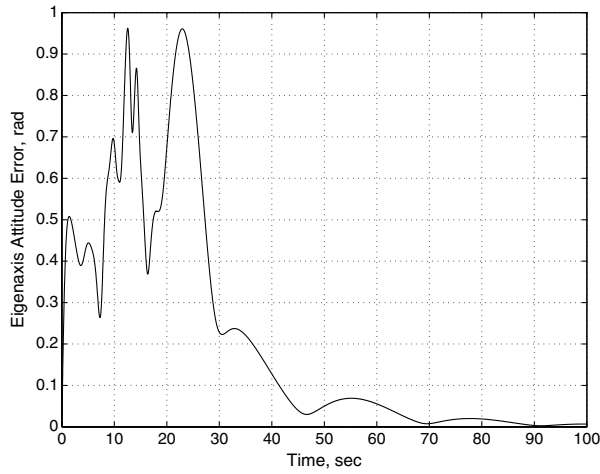
**Fig. 10** Slewing maneuver using the control law (53) under a disturbance that is constant with respect to the bus-fixed frame. The maximum rotation rate of each wheel is saturated at 100 rad/s.

100 rad/s, disturbance and inertia estimates diverge, and the system is destabilized.

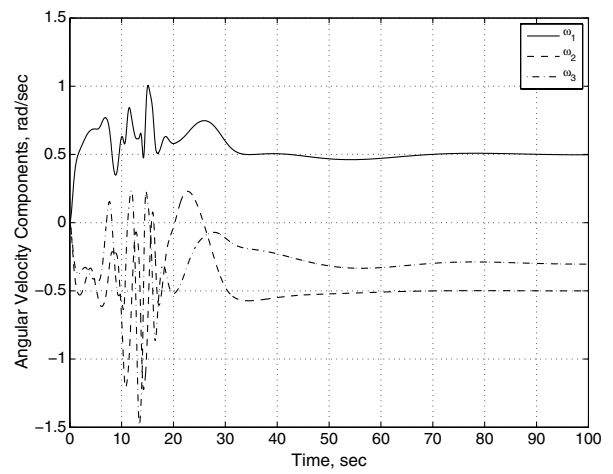
### C. Spin Maneuver Using Control Law (53)

Consider a spin maneuver with the spacecraft initially at rest and  $R(0) = I_3$ . The desired attitude is determined by  $R_d(0) = I_3$ , and the commanded constant angular velocity is  $\omega_d = [0.5 \ -0.5 \ -0.3]^T$  rad/s.

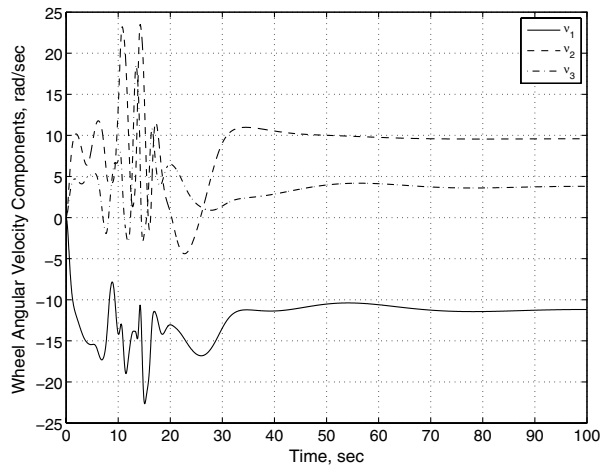
Assume no disturbance. Figures 11a–11f show, respectively, the attitude errors, angular-velocity components, angular rates of the wheels, the control inputs, which are the angular accelerations of the wheels, angular momentum, and inertia-estimate errors. For this maneuver, the spin command consists of a specified time history of rotation about a specified body axis aligned in a specified inertial direction. The controller achieves the commanded spin within about 100 s.



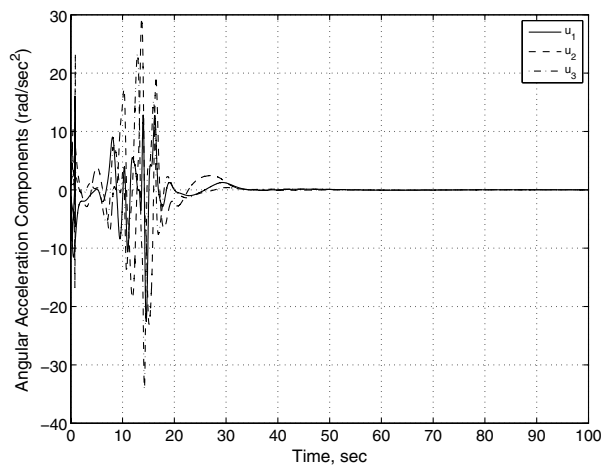
a) Eigenaxis attitude error



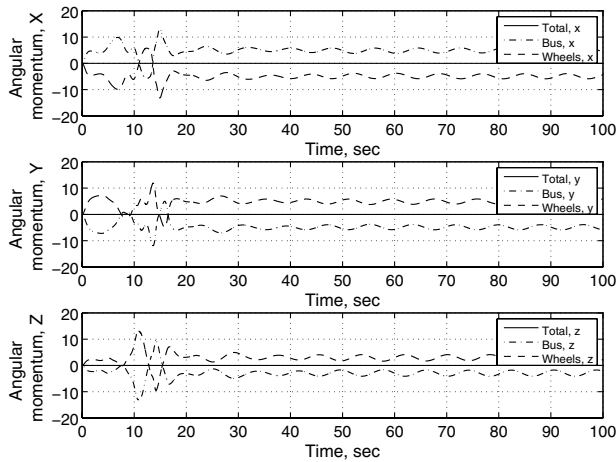
b) Spacecraft angular-velocity components



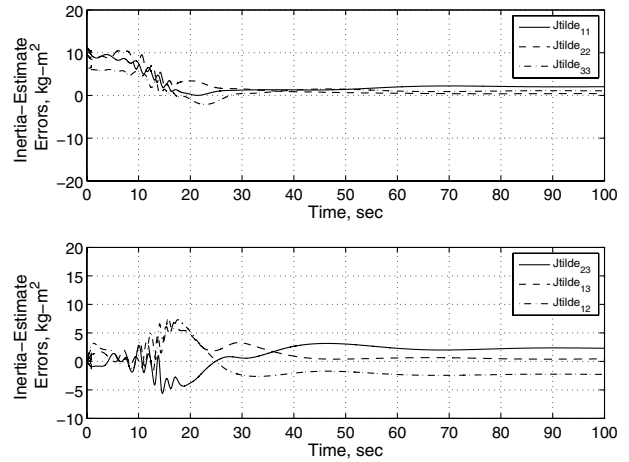
c) Angular rates of the reaction wheels



d) Angular accelerations of the reaction wheels



e) Angular momentum of the spacecraft relative to its center of mass with respect to the inertial frame resolved in the inertial frame



f) Inertia-estimate errors

Fig. 11 Spin maneuver using the control law (53).

### VI. Conclusions

Almost global stabilizability (that is, Lyapunov stability with almost global convergence) of spacecraft tracking is feasible without inertia information and with continuous feedback using three linearly independent reaction wheels, for which the axes of rotation are not necessarily aligned with the principal axes of the spacecraft bus, do not necessarily pass through the spacecraft's center of mass and are

not necessarily mass balanced in order to preserve the location of the spacecraft's center of mass. In addition, asymptotic rejection of harmonic disturbances (including constant disturbances as a special case) is possible with knowledge of the disturbance spectrum but without knowledge of either the amplitude or phase.

Under these assumptions, the adaptive control laws presented in this paper provide an alternative to previous controllers that 1) require

exact or approximate inertia information or 2) are based on attitude parameterizations such as quaternions that require discontinuous control laws or fail to be physically consistent (that is, specify different control torques for the same physical orientation). A future extension will address spacecraft actuation using control moment gyroscopes.

### Acknowledgments

The authors wish to thank Marc Camblor for generating Fig. 1 and the reviewers for their helpful comments.

### References

- [1] Junkins, J. L., Akella, M. R., and Robinett, R. D., "Nonlinear Adaptive Control of Spacecraft Maneuvers," *Journal of Guidance, Control, and Dynamics*, Vol. 20, No. 6, 1997, pp. 1104–1110.  
doi:10.2514/2.4192
- [2] Ahmed, J., Coppola, V. T., and Bernstein, D. S., "Adaptive Asymptotic Tracking of Spacecraft Attitude Motion with Inertia Matrix Identification," *Journal of Guidance, Control, and Dynamics*, Vol. 21, No. 5, 1998, pp. 684–691.  
doi:10.2514/2.4310
- [3] Sanyal, A., Fosbury, A., Chaturvedi, N., and Bernstein, D. S., "Inertia-Free Spacecraft Attitude Tracking with Disturbance Rejection and Almost Global Stabilization," *Journal of Guidance, Control, and Dynamics*, Vol. 32, No. 4, 2009, pp. 1167–1178.  
doi:10.2514/1.41565
- [4] Chaturvedi, N., Sanyal, A., and McClamroch, N. H., "Rigid Body Attitude Control: Using Rotation Matrices for Continuous, Singularity-Free Control Laws," *IEEE Control Systems Magazine*, Vol. 31, No. 3, 2011, pp. 30–51.  
doi:10.1109/MCS.2011.940459
- [5] Wie, B., and Barba, P. M., "Quaternion Feedback for Spacecraft Large Angle Maneuvers," *Journal of Guidance, Control, and Dynamics*, Vol. 8, No. 3, 1985, pp. 360–365.  
doi:10.2514/3.19988
- [6] Joshi, S. M., Kelkar, A. G., and Wen, J. T., "Robust Attitude Stabilization Using Nonlinear Quaternion Feedback," *IEEE Transactions on Automatic Control*, Vol. 40, No. 10, 1995, pp. 1800–1803.  
doi:10.1109/9.467669
- [7] Bhat, S. P., and Bernstein, D. S., "A Topological Obstruction to Continuous Global Stabilization of Rotational Motion and the Unwinding Phenomenon," *Systems and Control Letters*, Vol. 39, No. 1, 2000, pp. 63–70.  
doi:10.1016/S0167-6911(99)00090-0
- [8] Crassidis, J. L., Vadali, S. R., and Markley, F. L., "Optimal Variable-Structure Control Tracking of Spacecraft Maneuvers," *Journal of Guidance, Control, and Dynamics*, Vol. 23, No. 3, 2000, pp. 564–566.  
doi:10.2514/2.4568
- [9] Mayhew, C. G., Sanfelice, R. G., and Teel, A. R., "Quaternion-Based Hybrid Control for Robust Global Attitude Tracking," *IEEE Transactions on Automatic Control*, Vol. 56, No. 11, 2011, pp. 2555–2566.  
doi:10.1109/TAC.2011.2108490
- [10] Cortes, J., "Discontinuous Dynamic Systems," *IEEE Control Systems Magazine*, Vol. 28, June 2008, pp. 36–71.  
doi:10.1109/MCS.2008.919306
- [11] Levine, W. S., *Control Systems Applications*, CRC Press, Boca Raton, FL, 1999, p. 132.
- [12] Kasdin, N. J., and Paley, D. A., *Engineering Dynamics*, Princeton Univ. Press, Princeton, NJ, 2011.
- [13] Hughes, P. C., *Spacecraft Attitude Dynamics*, Wiley, 1986; reprint, Dover, New York, 2008, p. 17.
- [14] Koditschek, D. E., "The Application of Total Energy as a Lyapunov Function for Mechanical Control Systems," *Dynamics and Control of Multibody Systems*, Vol. 97, edited by Marsden, J. E., AMS, Providence, RI, 1989, pp. 131–157.
- [15] Cruz, G., Yang, X., Weiss, A., Kolmanovsky, I., and D. S. Bernstein, D. S., "Torque-Saturated, Inertia-Free Spacecraft Attitude Control," *AIAA Guidance, Navigation, and Control Conference*, AIAA Paper 2011-6507, portland, OR, Aug. 2011.